The Significance of coccolithophore blooms for the oceanic carbon cycle: A numerical modelling experiment simulating *Emiliania huxleyi* blooms in the North Atlantic

Report to "Schweizerischer Nationalfonds zur Förderung der Wissenschaftlichen Forschung", Period from April 1, 1993 to September 30, 1994.
Grant No. 8220-033288.

Michael Knappertsbusch

November 2, 1994

Abstract.

A one-dimensional seasonal mixed-layer model has been developed, which simulates modern blooms of siliceous (diatoms) and calcareous phytoplankton (coccolithophorids) at various latitudes in the Eastern North Atlantic. This investigation has been carried out in close collaboration with marine ecosystem modellers (Dr. A. Taylor and his group) at the Plymouth Marine Laboratory, U.K. (visit of the author at PML from November 1, 1993 to December 15, 1993), and with physiologists at the Netherlands Institute for Sea-Research (NIOZ) at Texel, NL. The model allows to study the dynamical behaviour of these algae under various environmental conditions and to calculate annual rates of organic carbon production and, in the case of the coccolithophorid *Emiliania huxleyi*, calcite production as well. It reproduces the succession of diatom- and *E. huxleyi* blooms and predicts reasonable values for cell concentrations, which are similar to those observed in nature. Bloom formation is triggered by the combination of a shoaling mixed layer, the increasing illumination, rising temperatures, low to moderate grazing pressure and high nutrient levels within the euphotic zone. The main limiting factor for the size and duration of the modeled diatom blooms is the amount of available silica in the mixed layer. Simulation experiments have shown, that diatom blooms often reach much higher standing stocks in terms of chlorophyll concentration than coccolithophorid blooms, which has also been observed under natural situations. The model nicely simulates the gradual increase in amplitude of diatom blooms as latitude increases, but with temporal retardement at high latitudes. In the case of coccolithophorids large blooms resulted around 47°N. The time of onset and the magnitude of *E. huxleyi* blooms are mainly determined by the amount of dissolved nitrate, which is left over after the end of the preceding diatom bloom and the grazing pressure. If applied to other latitudes, especially those around 60°N, where extensive blooms of *E. huxleyi* have frequently been detected from satellite imagery, the present model is not yet capable to reproduce large coccolithophore blooms. Presumably, large diatom blooms are one reason, because they remove most of the nitrate necessary for extended *E. huxleyi* blooms. Another reason for this failure might be a too simple concept of the hydrological structure of the watercolumn and the underwater light field during summer months (no winds included). The problem could eventually solved by replacing the simple three layer-structure by a quasi continuous vertical structure, which introduces local derivatives in the describing differential equations. Calculated vertically integrated annual rates of *E. huxleyi* coccolith calcite production at various latitudes ranges from about 2.5 to over 40 gr calcite m^{-2} yr^{-1}. Although these values are still too high when compared with measured fluxes of coccolith calcite in sediment traps (a global average is about 1.4 gr coccolith calcite m^{-2} yr^{-1}) they are already major improvements to earlier versions of the model.

Final report for the period April 1, 1993 to September 30, 1994, with the topic:

The significance of coccolithophore blooms for the oceanic carbor cycle: A numerical modelling experiment simulating *Emiliania huxleyi* blooms in the North Atlantic.

1. Introduction.

On a global scale burning of fossil fuels has been estimated to be about 5.4 Gt C yr^{-1} (1 Gt equals to 10^9 tons), which, together with the effects of deforestation (1.6 Gt C yr^{-1}), amounts to a total emmission of 7.0 Gt C into the atmosphere every year. Counteracting to this anthropogenic input of C into the atmosphere there are the absorption of CO_2 by the oceans (about 2.0 Gt C yr^{-1}) and the uptake of CO_2 by terrestrial plants (1.7 Gt C yr^{-1} ?), but still there remain about 3.3 Gt C annually, which are continuously accumulate in form of CO_2 in the atmosphere since the industrial revolution. Because of their size and their ability to act as a dynamic carbon reservoir oceans play an outstanding role for the evolution of the modern climate. For example, the modern global ocean export production of organic C has been estimated to amount to 5 Gt yr^{-1} (range: 3-6 Gt yr^{-1}), most which (98% to 99%), however, is almost immediately remineralized in the watercolumn or at the sediment water interface. A permanent removal of carbon from the ocean-atmosphere system over long time occurs through the export production of biogenic calcite carbon. At present it has been estimated, that the export production of biogenic calcite amounts at least 0.64 Gt C yr^{-1} (range: 0.64-2.0 Gt C yr^{-1}). At least 42% of the global annual biogenic calcite export production comes through marine planktonic calcifying organisms - foraminifera, pteropods and coccolithophorids - with an average export production of 0.29 gigatons of calcite carbon each year (Milliman, 1993). Coccolithophorids, which are a major group of calcifying algae, export about 0.049 gigatons calcite carbon per year from the euphotic zone to the interior of the oceans, which is about 17 % of the global annual pelagic calcite production. These figures illustrate, that calcite carbon production and its deposition in deep sea sediments are of great interest for a better understanding of the efficiency of the oceans as a carbon pump over timescales of a few hundred to thousands of years.

In this context the frequent occurrence of extended blooms of the coccolithophore *Emiliania huxleyi* gave rise to the hypothesis, that calcifying algae play an important role in changes of atmospheric CO_2 levels. Yet, reliable data on measured fluxes of coccolith calcite are still very poorly available. The situation becomes even more difficult, when the few

sediment trap measurements of coccolith fluxes are compared with coccolith calcite production rates, which were derived from satellite imagery. For example, Brown and Yoder (1994) concluded from a global and multi-year survey of coccolith blooms in satellite images, that coccolithophorids may produce between 0.00056 to 0.0018 gigatons calcite carbon per year, which deviates from measured fluxes by at least one order of magnitude.

To obtain an alternative tool to arrive at better estimates of carbonate production by calcareous phytoplankton in the modern oceans, I have started to develop a computer model, which allows to calculate coccolith calcite production rates from physiological and environmental data. The goal was to develop a seasonal production model of *E. huxleyi* for the Eastern North Atlantic on the basis of population dynamics and from known environmental and physiological parameters for this species, which later can be implemented in a more general circulation or ecosystem model, and which can then also be extended to other areas of the oceans.

2. Description of the model:

2.1. General structure of the model (program COCDIA):

The model consists of three layers, a mixed layer M with thickness H_m at the surface, a thermocline layer T below with thickness H_t and a "bottom layer" B, which has an unlimited thickness (Figure 1). In the following, the subscripts m, t and b refer to these three layers. H_m varies seasonally, while H_t is kept at a constant thickness. The light intensity varies also with season and latitude and includes a daily light-dark cycle with varying durations of the illumination period depending on time and location. Of the 38% photosynthetically available radiation (PAR, 400nm-700nm) within the spectrum of solar radiation a fraction is attenuated to various degrees within the atmosphere due to absorption, reflection and backscattering within clouds and by dry air molecules, dust and water vapour, all of which depend on the latitude. Of the transmitted solar radiation another portion is reflected at the air-water interface (the sea-surface albedo), which also varies with season and latitude. The water entering solar radiation is splitted into three equally wide wave-bands of red, green and blue light (indicated by subscripts r, g and b, respectively), each band obeying the exponential decay function as is described by the law Lambert-Beer, but with different extinction coefficients. The extinction coefficients depend on the concentrations of suspended particles.

Two phytoplankton groups, coccolithophorids (P) and diatoms (D) are included, which are growing in the mixed and thermocline layers with growth rates G_p and G_d, respectively. For the bottom layer it is assumed, that no growth occurs and phytoplankton concentrations remain constant. Growth of phytoplankton is by cell division. All cells of a particular species are identical in size and populations have no age structure. Nutrients included are dissolved nitrate (N) and silicate (S). Coccolithophorids depend only on nitrate, while diatoms take up nitrate and silicate.

Coccolithophorids are calcifying at a rate Γ and produce "attached liths" (L_a), which form the coccosphere. Although in reality coccolithophorid biomass (P) and attached liths (L_a) belong to the same individual and form a single particle, they are treated as two separate components in the model. However, P and L_a are interconnected by cell-growth and per cell coccolith formation, and sink and mix together in the watercolumn.

Coccolithophorids are allowed to detach parts of their coccosphere into the water as has often been observed in *Emiliania huxleyi,* and the isolate liths are treated as "free liths" (L_f). The rate of coccolith detachment R_{det} is modeled as a function of the ratio of attached liths per cell (Q).

All suspended particles (P, D, L_a and L_f) and dissolved nutrients (N and S) are assumed to be homogeneously distributed in each layer. The mixed and thermocline layers, and the thermocline and bottom layers exchange phytoplankton cells, free and attached liths and nutrients through turbulent mixing, which depends on the gradient of components between two adjacent

layers. Turbulent mixing between the surface mixed layer and the thermocline layer is controlled by mixing constant K_2 and mixing between the thermocline layer and the bottom layer by constant K_1. To introduce seasonal variation of turbulent mixing between the layers, K_1 and K_2 are modulated by the thickness of the mixed layer. Nutrients in the bottom layer vary linearly with depth and latitude.

Living cells of coccolithophorids (P and L_a together) as well as diatoms are sinking through the watercolumn at constant settling rates (V_{coc} and V_{dia}, respectively), while free liths, which are very small, remain in suspension and do not settle down.

Grazing of coccolithophorids and diatoms by zooplankton are treated as a loss term, without explicit calculation of a grazing population. The intrinsic grazing rates for coccolithophorids and diatoms in the mixed layer and the thermocline layers ($M_{c,m}$, $M_{c,t}$ and $M_{d,m}$, $M_{d,t}$, respectively) are sinusoidal functions to mimic seasonal variation of grazing zooplankton. The resulting loss terms for coccolithophorids and diatoms are the products of the density of a phytoplankton species times the respective intrinsic grazing rates M_c or M_d, respectively. Grazing includes the ingestion of attached liths on a coccosphere and the ingestion of free liths ("sloppy feeding").

With these parameters, the change of each component with time (t) is described by the following set of differential equations:

Mixed layer:

Coccolithophorids:

$$dP_m/dt = (G_{p,m} - M_{c,m} - V_{coc}/H_m)*P_m + K_2*(P_t-P_m)/H_m$$

Diatoms:

$$dD_m/dt = (G_{d,m} - M_{d,m} - V_{dia}/H_m)*D_m + K_2*(D_t-D_m)/H_m$$

Nitrate:

$$dN_m/dt = -\gamma_p*(G_{p,m} - \varepsilon_{coc}*M_{c,m})*P_m - \gamma_d*(G_{d,m} - \varepsilon_{dia}*M_{d,m})*D_m + K_2*(N_t-N_m)/H_m$$

Silicate:

$$dS_m/dt = -\gamma_d*G_{d,m}*P_m + K_2*(S_t - S_m)/H_m$$

Attached coccoliths:

$$dL_{a,m}/dt = P_m*Chl_{pc}*\Gamma_m - R_{det}*P_m*Chl_{pc} - M_{c,m}*L_{a,m} - V_{coc,m}*L_{a,m}/H_m + K_2*(L_{a,t}-L_{a,m})/H_m$$

Free liths:

$$dL_{f,m}/dt = R_{det}*P_m*Chl_{pc} - M_{c,m}*L_{f,m} + K_2*(L_{f,t}-L_{f,m})/H_m$$

Thermocline layer:

Coccolithophorids:

$$dP_t/dt = (G_{p,t} - M_{c,t}) - V_{coc}*(P_t-P_m)/H_t + K_1*(P_b-P_t)/H_t - K_2*(P_t-P_m)/H_t$$

Diatoms:

$$dD_t/dt = (G_{d,t} - M_{d,t})*D_t - V_{dia}*(P_t-P_m)/H_t + K_1*(D_b-D_t)/H_t - K_2*(D_t-D_m)/H_t$$

Nitrate:

$$dN_t/dt = -\gamma_p*(G_{p,t} - \varepsilon_{coc}*M_{c,t})*P_t - \gamma_d*(G_{d,t} - \varepsilon_{dia}*M_{d,t})*D_t + K_1*(N_b-N_t)/H_t - K_2*(N_t-N_m)/H_t$$

Silicate:

$$dS_t/dt = -\gamma_d*G_{d,t}*P_t + K_1*(S_b-S_t)/H_t - K_2*(S_t - S_m)/H_t$$

Attached coccoliths:

$$dL_{a,t}/dt = P_t*Chl_{pc}*\Gamma_t - R_{det}*P_t*Chl_{pc} - M_{c,m}*L_{a,t} - V_{coc}*(L_{a,t}-L_{a,m})/H_t + K_1*(L_{a,b}-L_{a,t})/H_t - K_2*(L_{a,t}-L_{a,m})/H_t$$

Free liths:

$$dL_{f,t}/dt = R_{det}*P_t*Chl_{pc} - M_{c,t}*L_{f,t} + K_1*(L_{f,b}-L_{f,t})/H_t - K_2*(L_{f,t}-L_{f,m})/H_t$$

In these equations γp and γd are conversion factors to express the organic carbon content of coccolithophorid and diatom chlorophyll in units of nitrogene and silicate, respectively. Implicitely, γp and γd include a cellular organic carbon to chlorophyll ratio of 40. The parameters ε_{coc} and ε_{dia} indicate the efficiencies of nitrogene remineralization in coccolithophorids and diatoms, respectively, and vary from 0 (no nitrogene remineralization) to 1 (complete nitrogene remineralization). The model does not consider silica remineralization from diatom shells. Chl_{pc} is the inverse of the chlorophyll content per cell in coccolithophorids.

2.2. Phytoplankton growth:

Coccolithophorid and diatom growth depends on the ambient light (I) and temperature (T), which both vary with time and waterdepth, and the dissolved nutrients (N and S). For both phytoplankton groups the growth rates G are assumed to be products of a maximum potential growth rate G_{max}, which depends on the temperature (T), a light dependent factor α, and a nutrient dependent factor Φ:

For coccolithophorids (in day^{-1}): $G_p = G_{maxe}(T)*\alpha_p(I)*\Phi_p(N)$

For diatoms (in day^{-1}): $G_d = G_{maxd}(T)*\alpha_d(I)*\Phi_d(N,S)$

The terms $G_{maxe}(T)$ and $G_{maxd}(T)$ describe the maximum potential growth rates at a particular temperature and under light and nutrient saturation for *E. huxleyi* and diatoms, respectively. The terms Φ and α are scaling functions, which can reach values between 0 and 1, depending on nutrients or light intensities.

2.2.1 Influence of temperature on growth rates:
Temperature has a strong influence on phytoplankton growth. Eppley (1972) and Goldman and Carpenter (1974) provided experimental evidence, that the maximum potential growth rate G_{max} of a variety of marine and limnic phytoplankton species follow a fundamental law, which can be described by the Arrhenius equation in the form of

$$G_{max}=A*Exp(-E/(R*T))$$

In this equation A is a constant, E is the activation enery for an enzymatic reaction, R is the universal gas constant and T is the temperature (Kelvin scale). According to Goldman and Carpenter (1974) the constant A is $5.35x10^9$, and the ratio E/R is 6472. With these values G_{max} would follow the van't Hoff rule, which predicts an approximate doubling of a biological reaction rate for each 10°C rise in temperature. A review of literature data (Mjaaland, 1956; Watabe and Wilbur, 1966; Brand and Guillard, 1981; Brand, 1982; Fisher and Honjo, 1991; Balch et al., 1992; van Bleijswijk et al., 1994) on culture experiments under varying conditions has shown, that this model is only roughly valid for *E. huxleyi* and only at temperatures below 15°C (Figure 2). Outside that range the maximum potential growth deviates strongly from measured average growth rates. For this reason the maximum potential growth rate for diatoms and coccolithophorids are treated in two separate ways: For diatoms the model of Goldman and Carpenter has been implemented. The temperature dependency of *E. huxleyi* growth follows a parametrized curve derived from laboratory measurements done by Lesley, Harris and Conte (presented during the fifth GEM Meeting in 1994), with optimum growth between about 17°C and 25°C and with non-zero growth between 6°C to 30°C. Outside the temperature tolerance range (i.e. 6°C and 30°C) growth is set to zero (Figure 2, curve "GEM Meeting 1994").

2.2.2 Light dependent growth:
Photosynthesis-irradiance (P-I) functions in coccolithophorids and diatoms are both assumed to follow a non-linear function of the form

$$\alpha(I) = G_{max}*(1-Exp(-a*I/G_{max}))$$

This model has first been proposed by Webb et al. (1974) for the CO_2 exchange of *Alnus rubra* (see also Henley (1993) for a review of P-I curves in algae) and has been proposed by Balch et al. (1992) to describe the light dependent photosynthetic carbon assimilation rate in *E. huxleyi*. G_{max} is the maximum potential carbon assimilation rate (i. e. the carbon assimilation rate under light and nutrient saturation and at optimum temperatures), I is the light intensity and a is the absorption coefficient for chlorophyll. For our purpose we have adopted the scaling function

$$\alpha(I) = (1-Exp(-a*I/G_{max}))/C_{cpc}$$

to describe the response of algal growth to changing light intensities. C_{cpc} stands for the organic carbon content of an individual diatom or coccolithophorid cell (which are both assumed to be constants) and relates the photosynthetic carbon uptake to the different cell sizes of these two phytoplankton groups. Note, that G_{max} is a function of temperature and is different for diatoms and coccolithophorids in the present model.

2.2.3 Nutrient dependent growth:

If nutrients become limiting, growth will cease, and for both phytoplankton groups Φ is assumed to follow the Michaelis-Menten uptake kinetics. In the case of diatoms, which depend on dissolved nitrate (N) and silicate (S), the concept of "limiting factors" of Liebig is applied: Φ_d is calculated from nitrate and silicate separately, and then the smaller of the two values is taken. The influence of nutrient limitation on the growth rates for coccolithophorids and diatoms can then be formulated by:

Coccolithophorids:	$\Phi_p(N) = N/(N+\nu chalf)$
Diatoms:	$\Phi_d(N,S) = Min\{N/(N+\nu shalf), S/(S+\nu dhalf)\}$

The constants $\nu chalf$, $\nu dhalf$ and $\nu shalf$ are the half saturation constants for nitrate dependent growth in coccolithophorids, and nitrate and silicate dependent growth of diatoms, respectively. The notation Min{a,b} means the smaller value of experessions a and b. If nutrients are limiting Φ will range between 0 and 1.0, and under conditions of nutrient saturation Φ will approach 1.0. In figure 3 an example is illustrated for the change of the specific growth rate of *E. huxleyi* (Gp) with changing nitrate concentrations under 9 different combinations of temperature and light intensity.

2.3. Calcification

3.1 Production of coccoliths

It is assumed, that in an *E.huxleyi* population coccolith production is identical for all cells. The production of new coccoliths per cell cell (attached coccoliths, L_a) is therefore calculated as the product of cell concentration ($=P^*Chl_{pc}$) times the per cell rate of coccolith production (Γ), which can be described by the differential equation

$$dL_a/dt = P^*Chl_{pc}^*\Gamma$$

Similar to the rate of photosynthetic carbon uptake the rate of carbon assimilation into coccoliths of *E. huxleyi* (Γ') depends on the light intensity (Figure 4). Balch et al. (1992) have proposed the formula

$$\Gamma'=C'_{cmax}*[(1-Exp(-a_c*I/C'_{cmax})+C'_{dar}]$$

Γ' is the carbon uptake rate into coccoliths, C'_{cmax} is the maximum carbon assimilation rate into coccoliths, a_c is the light absorption coefficient for saturated calcification and C'_{dar} is the assimilation rate of carbon into coccoliths in the absence of light. The apostroph " ' " indicates, that assimilation rates are given in fmol C hr^{-1} $cell^{-1}$. The rate of coccolith production per cell Γ, which is in coccoliths day^{-1} $cell^{-1}$, is then obtained by multiplication of Γ' with the C content per coccolith.

2.3.1. Detachment of coccoliths

In natural blooms *E. huxleyi* has frequently been observed to detach coccoliths from their cells into the water, which can severely reduce the thickness of the illuminated part of the mixed layer and therefore strongly lowers the photosynthetic growth of phytoplankton. Because reasons and mechanisms for coccolith detachment are not well understood at all, the release of isolated coccoliths (L_f) into the water has been modeled by a very simple differential equation of the form

$$dL_f/dt = R_{det}*P^*Chl_{pc}$$

This equation says, that the increase of suspended liths with time is proportional to the product of the number of cells present at that time ($=P^*Chl_{pc}$) times a rate of coccolith detachment per cell (R_{det}). From light microscopic examinations of living cells there is evidence, that the maximum number of attached coccoliths on a cell (Q_{max}) for *E. huxleyi* is about 80 to 100 (Van der Wal, personal communication, Balch et al., 1993, own observations). I suggest, that R_{det} depends on the number of attached coccoliths per cell (Q), which itself depends on the rate of calcification and the growth rate. Assuming, that coccolith detachment increases as cells develop multilayer coccospheres, and that the maximum number of

coccoliths per cell reaches an upper limit, where the coccosphere tends to decay, then the rate of detachment can be tentatively formulated by

$$R_{det}=R_{deto}*\tan(\pi*Q/Q_{max})$$

with $Q=L_a/(P*Chl_{pc})$ and R_{deto} being a constant (Figure 5).

2.4. Light

The vertical distribution of the light intensity in water follows the law of Lambert-Beer, which is of the form

$$I(H)=I_{surf}*Exp(-K_{ex}*H)$$

I_{surf} is the incident light intensity at at sea-surface, K_{ex} is the diffuse attenuation coefficient (which is a composite of constants for clear water, dissolved substance and suspended matter) and H is the thickness of the watercolumn. In the model it is assumed, that photosynthesis and calcification depend on the average light intensity in a respective layer, and that within a layer the vertical distribution of light is uniform. For a given layer X with thickness $H_X(t)$ the light intensity at time t is then:

$$I_X = 1/H_X(t)*\int_{z_1}^{z_2} I_{surf}(t)*Exp(-K_{ex}*z)dz$$

where z_1 and z_2 are the upper and lower depths of layer X.

2.4.1 Calculation of the incident light at sea-surface:

The total irradiance from the sun reaching the sea-surface is calculated as a function of time, latitude and astronomical parameters with the method described in Sellers (1965). Figure 6 shows an example of the solar radiation at sea-surface and the light intesity in the mixed and thermocline layers at solar noon, and Figure 7 illustrates the course of the solar radiation penetrating the sea-surface during a single day (January 6) at 47°N.

For the solar irradiation a zonal correction term for absorption and reflection of light due to clouds, air molecules, dust and water vapour data from Sellers (1965) have been used (Figures 8.a-c). To include the seasonal and latitudinal variation of the sea-surface albedo a data set from Goldsmith and Bunker (1979) has been implemented (Figures 9.a-b).

As light enters the sea-surface, about 50% (infrared) is lost in the first centimeter (Taylor et al., 1990). In reality there are continuous spectra for

absorption and scattering of light due to water and suspended or dissolved constituents. At present there are not yet enough experimental observations available to completely describe such a natural situation and simplifications have to be made. In the present model it is assumed, that the light, which penetrates the surface skin of the oceans, can be subdivided into three wave-bands, a red one (800-650nm), a green (650-500nm) and a blue (500-400nm) one, each with different extinction coefficients. With other words, a third of the irradiance, that is not absorbed at the surface is assumed to be red light, for which the extinction coefficient is

$$K_{exr}=0.4 + 0.016*(P+D),$$

one third is green light with an extinction coefficient of

$$K_{exg}=a_g + b_g$$

and one third is blue light with the extinction coefficient of

$$K_{exb}=a_b + b_b$$

(because there are no data on absporption or backscatter due to coccoliths in the red band, K_{exr} has only been calculated as a function of chlorophyll concrentrations). In these equations a_g,a_b and b_g,b_b are the total absorption coefficients and total backscatter coefficients for green and blue light respectively, all of them being functions of the chlorophyll and coccolith concentrations in the water. In our model and applying the experimental results for *E. huxleyi* shown in Balch et al. (1991) these coefficients can be formulated in the following way (at 550nm):

$$a_g=1.17\times10^{-11}* (P+D) + a_{wg}$$

$$b_g=b'_{bg} + 0.54\times10^{-11} * (P+D) + b_{bwg}$$

and with $$b'_{bg}=1.28\times10^{-3} + 1.29\times10^{-7}*LF - 8.4\times10^{-14}*LF^2$$

P and D are the chlorophyll concentrations of coccolithophorids and diatoms in mg Chla m^{-3} and LF is the concentration of coccoliths in the water (in Liths ml^{-1}). The constants awg and bbwg are the absorption and backscatter coefficients for green light for water in absence of chlorophyll and coccoliths and have been taken from Jerlov (1968). b'_{bg} is the coccolith backscatter for green light as a function of coccolith concentration.

The total absorption and backscatter coefficients for blue light (436nm) can be calculated in a similar way, i.e.

$$a_b = 5.62 \times 10^{-11} * (P+D) + a_{wb}$$

$$b_b = b'_{bb} + 2.18 \times 10^{-11} * (P+D) + b_{bwb}$$

and $$b'_{bb} = 3.24 \times 10^{-3} + 1.41 \times 10^{-7} * LF - 5.27 \times 10^{-14} * LF^2$$

2.4.2 Light intensity in the mixed and thermocline layers:
Applying the formulae above the average light intensity available for photosynthesis and calcification in the mixed layer is then

$$I_m = I_{surf}(t)/(6*H_m(t)) * \int_{z=0}^{z=H_m(t)} [Exp(-K_{exr}*z) + Exp(-K_{exg}*z) + Exp(-K_{exb}*z)]dz$$

and for the thermocline layer

$$I_t = I_{surf}(t)/(3*H_t) * \int_{z=H_t}^{z=H_m(t)+H_t} [Exp(-K_{exr}*z) + Exp(-K_{exg}*z) + Exp(-K_{exb}*z)]dz$$

Because of a homogeneous distribution of phytoplankton and coccoliths (no variation with depth) in a single layer these integrals can easily be solved analytically (not shown here). See Figure 6 for a simulated example of the annual course of I_m and I_t.

2.5. Seasonal variations of temperature:
Seasonal temperature (T) variation was calculated as proposed by Taylor et al. (1990). It follows a sine of the form

$$T = T_{min} + 0.5*(T_{max} - T_{min})*[1 + \sin(2*\pi*(t-135.75)/365)]$$

T_{max} and T_{min} are maximum and minimum temperatures during a year and t is the time in days. Figure 10 illustrates the temperature variations in the mixed and thermocline layers at 47°N.

2.6. Seasonal variations of the mixed layer thickness:
The seasonal variation of the mixed layer (H_m) was parametrized from monthly maps of the average depth to the top of the thermocline published by Robinson et al. (1979). For the 20°W transect reference points were selected between 35°N and 60°N at intervals of 5° latitude (Figure 11).

2.7. Latitudinal and vertical variation of nitrate and silicate in the bottom layer:

Because nutrients show strong gradients with latitude and depth (below the thermocline layer), a simple linear parametrization of nutrients has been constructed from field data (see Figures 12.a,b in the case of nitrate). At a single location N_b and S_b vary with depth according to

$$N_b=a^*(H_m+H_t)+b$$
$$S_b=c^*(H_m+H_t)+d$$

The coefficients a,b,c and d are functions of latitude only, while H_m+H_t is a function of latitude and time (Figures 13.a,b). The data to derive these coefficients where from APNAP II and JGOFS cruises in the Eastern North Atlantic. Figure 13.c illustrates the seasonal variation of dissolved nitrate and silicate concentrations in the bottom layer at 47°N obtained in that way.

2.8. Seasonal variation of mixing coefficients.

The vertical mixing coefficients K_1 and K_2 are small when the density stratification is intense (i.e. weak mixing accross the boundary) and larger (i.e. strong mixing accross the boundary) if the vertical homogeization is strong.

$$K_1=K_{1s}^*(H_M/25.0)\text{exp}1.5$$
$$K_2=K_{2s}^*(H_M/25.0)\text{exp}1.5$$

The same values as in Taylor et al. (1991) are used here too.

2.9. Seasonal variation of grazing of diatoms and coccolithophorids:

The intrinsic grazing rates (in day^{-1}) in the mixed and thermocline layers for diatoms and coccolithophorids ($M_{d,m}$, $M_{d,t}$, and $M_{c,m}$, $M_{c,t}$, respectively) are calculated by a sinuisoidal function (after Taylor et al., 1991)

$$M=M_{min}+0.5^*(M_{max}-M_{min})^*(1.0+\sin(arg))$$

with the argument

$$arg=2.0^*\pi^*(t-135.75)/365.0$$

M_{min} and M_{max} are the minimum and maximum grazing rates during the annual cycle and t is the time.

2.10. Annual production of organic and inorganic carbon (program PPP400):

The vertically and annually integrated production of calcite ond organic carbon in the euphotic zone is calculated in a separate program (program PPP400). The daily production of C_{org} per *E. huxleyi* cell during a very small time interval dt and within a volume element dV=A*dz (where A is the bottom area and dz is the height of that volume element) is equal to

$$G_{maxe}(T)*\alpha_p(I)*\Phi_p(N)*dt*dV/A$$

Because production occurs only within the photic zone, we have to integrate over the depth of the photic zone H_p. Then, and using a "unity-watercolumn" with a bottom area of A=1 m^2 the production for all cells in the photic zone during that time-interval becomes

$$\int_{z=0}^{z=H_p(t)} G_{maxe}(T)*\alpha_p(I)*\Phi_p(N)*P(t,z)*dt*dz = G_{maxe}(T(t))*\alpha_p(I(t),T(t))*\Phi_p(N(t))*H_p(t)*dt$$

The annual production of organic carbon for *E. huxleyi* in the mixed layer, for example, is then

$$\int_{t=0}^{t=364} G_{maxe}(T(t))*\alpha_p(I(t),T(t))*\Phi_p(N(t))*H_p(t)*P_m(t)*dt$$

The total annual production of organic carbon over the entire euphotic zone is then the sum of the org C production of diatoms and *E. huxleyi* in the mixed and that part of the euphotic zone, which penetrates the thermocline layer. The annual production of *E. huxleyi* coccolith carbonate can be calculated in a similar way. The integration is performed with the trapezoidal rule using integration intervals of one day.

To determine the thickness of the euphotic zone (=H_p) as a function of time the decrease of the incident irradiation with depth is considered (see above). The photosynthetically available radiation in the mixed layer is

$$PAR_m(z)=I_{surf}*[Exp(-K_{exr,m}*z)+Exp(-K_{exg,m}*z)+Exp(-K_{exb,m}*z)]/6$$

The depth of the photic zone H_p can be calculated by setting

$$I_m(H_p)=0.01*PAR_m(0)$$

i.e. the depth of the photic zone is set at the depth of the 1% surface isolume. In the case that the depth of the photic zone penetrates the the thermocline layer, Hp is determined by solving the equation

$$IT(Hp)=I_{surf}*[Exp(-K_{exr,m}*H_m)+Exp(-K_{exg,m}*H_m)+Exp(-K_{exb,m}*H_m)]*$$
$$[Exp(-K_{exr,t}*z)+Exp(-K_{exg,t}*z)+Exp(-K_{exb,t}*z)/18 \leq 0.01*PAR$$

for H_p. The expressions $K_{exr,m}$, $K_{exg,m}$, $K_{exb,m}$, and $K_{exr,t}$, $K_{exg,t}$, $K_{exb,t}$ are the extinction coefficients for red, green and blue light in the mixed and thermocline layers, respecively. H_p is the used as the upper limit in the above integration.

3. Technical documentation of the code:

The model was written on a Macintosh Quadra 800 (8 Mb Ram, 230 Mb Harddisk, 33 Mhz, 68040 processor). The programming language was Fortran 77, and the compiler was Microsoft Fortran version 2.2 by Absoft. With this setup a one year simulation with a time step of one hour (=0.0416 days) takes about 15 minutes to run.

The programming environment of the model is illustrated in Figure 14. It is composed of three applications, which are COCDIA1004, PPP400 and REDUCE2. COCDIA 1004 and PPP400 require the include file COCDAT.inc, where constants and environmental parameters are stored. In addition COCDIA1004 needs the files MIXED_LAYER_DEPTHS, SEA_SURFACE_ALBEDO and ATM_COR, where data on the mixed layer depths, sea-surface albedo and zonal atmospheric corrections for incoming solar radiation are stored, respectively. The initial conditions of a simulation are stored in the external file INITCON.DAT. All files can be modified with the fortran editor for a particular simulation.

Running the model the program COCDIA1004 requires first the duration of the simulation from the keyboard. It then produces hourly data sets for all variables and components, which are written to the three output files LIGHT.DAT, PHYSICS.DAT, and PLANKTON.DAT. Because of the implementation of a diurnal light-dark cycle it was necessary to generate output files of at least every half day's resolution. Once a simulation is finished these three files serve as input into program PPP400 for the calculation of annual production rates of organic carbon and calcite. Output of PPP400 is a single file with cumulative production rates of organic carbon (ORGC, in gr C m^{-2}) and calcite (CALCITE, in gr calcite m^{-2}), given at hourly intervals. The program REDUCE2 is a tool to reduce the hourly data matrices to smaller data files (for example output for every day), which are more convenient to import into Cricket Graph for the production of graphs.

Formats of input files:

MIXED_LAYER_DEPTHS:
The first column contains the latitudes in degrees (decimal).
The second and the last column contains the depth of the base of the mixed layer (in meters) at January 1 and December 31. The other column contain the mixed layer depths (in meters) during mid month from January, February,

March, . . ., December. For example, column 3 contains the mixed layer depth at January 15.

SEA_SURFACE_ALBEDO:

The first column contains the latitudes in degrees (decimal). Northern latitudes are positive, southern latitudes are negative. The second and last columns contain the sea-surface albedo at begin of January and the end of December, respectively, which were interpolated from monthly means published in Goldsmith and Bunker, 1979. The other columns contain the monthly means for the sea-surface albedos for January, February, . . ., December.

ATM_COR:

The first column contains the latitudes (decimal, latitudes of the northern hemisphere are positive, those of the southern hemisphere are negative). Columns two to five represent correction factors as the solar radiation is reduced by absorption within clouds (C_a), reflection and backscattering by clouds (C_r), absorption by dry air molecules, dust and water vapour (A_a) and reflection and backscattering to space by dry air molecules, dust and water vapour (A_r), respectively. The atmospheric correction at the top of the atmosphere has the value 1.0, and reduces to values between 0 and 1.0 as light penetrates the atmosphere.

INITCON.DAT:

This file contains the initial conditions for a simulation. The first, second and third rows represent the initial conditions in the mixed layer, thermocline layer and the bottom layer, respectively. For each layer, the rows indicate the initial concentrations of coccolithophorid cells (PM,PT,PB, in mg Chla m^{-3}), attached coccoliths (LAM,LAT,LAB, in liths m^{-3}), suspended isolated coccoliths (LFM,LFT,LFB, in liths m^{-3}), dissolved nitrate (NM,NT,NB, in mM m^{-3}) and dissolved silicate (SM,ST,SB, in mM m^{-3}).

Formats of output files:

The extensions .DAT and .RED indicate hourly data sets and reduced data sets, respectively.

LIGHT.DAT and LIGHT.RED:

The columns represent in the following order:

TIME (in days): the actual time.

ISURF (in Wm^{-2}): the instantaneous flux of the photosynthetically available radiation (PAR) of the solar radiation, which penetrates the sea-surface.

LIGHTM, LIGHTT (in Wm^{-2}): the intensity of PAR in the mixed and thermocline layers, respectively.
TEMPM,TEMPT (in °C): The temperatures in the mixed and thermocline layers.
KEXRM, KEXGM,KEXBM,KEXRT,KEXGT,KEXBT (in m^{-1}): The extinction coefficients for red, green and blue light in the mixed and thermocline layers, respectively.

PHYSICS.DAT and PHYSICS.RED:
TIME (in days): the actual time.
HM and HP (in m): The depths of the mixed layers and the photic zone (1% isolume).
MALPHAC,TALPHAC,MALPHAD,TALPHAD (no units): The part of the growth rate, which is due to the light intensity for coccolithophorids in the mixed and thermocline layers (MALPHAC,TALPHAC) and for diatoms in the mixed and thermocline layers (MALPHAD,TALPHAD). Under light saturations these values approach to 1.0.
PHICM,PHICT,PHIDM,PHIDT (no units): The part of the growth rate, which is due to nutrient concentrations for coccolithophorids in the mixed and thermocline layers (PHICM,PHICT) and for diatoms (PHIDM,PHIDT) in the mixed and thermocline layers, respectively. Under nutrient saturation these values approach to 1.0.
GMXME,GMXTE,GMXMD,GMXTD (in day^{-1}): The maximum potential growth rates as a function of temperature of *E. huxleyi* in the mixed and thermocline layers (GMXME,GMXTE) and of diatoms in the mixed and thermocline layers (GMXMD,GMXTD), respecitively.
CALCM,CALCT (in Lith $cell^{-1}$ day^{-1}): The rate of calcification of *E. huxleyi* per cell and per day in the mixed and thermocline layers, respectively.

PLANKTON.DAT, PLANKTON.RED:
TIME (in days): the actual time.
PM,PT,DM,DT (in mg Chla m^{-3}): The concentrations of coccolithophorid cells (PM,PT) and diatom cells (DM,DT) in the mixed and thermocline layers, respectively.
LAM,LAT,LFM,LFT (in Lith m^{-3}): The concentrations of attached (LAM,LAT) and isolate (LFM,LFT) coccoliths in the mixed and thermocline layers.
NM,NT,SM,ST,NB,SB (in mM m^{-3}): The concentrations of dissolved nitrate (NM,NT,NB) and silicate (SM,ST,SB) in the mixed, thermocline and bottom layers, respectively.

PRODUCTION.DAT, PRODUCTION.RED:
TIME (in days): the actual time (=start of the integration interval).
TIMEN (in days): The time at the end of the integration interval.

CALCIT (in gr Calcite m^{-2}): Cumulative rate of the vertically integrated coccolith calcite production.
ORGC (in gr C m^{-2}): Cumulative rate of the vertically integrated organic carbon production by coccolithophorids and diatoms.

4. Preliminary results.

4.1. Model runs at a single location (47°N/20°W).

Diatom and coccolithophore blooms are triggered by the combination of a shoaling mixed layer, increasing illumination, rising temperatures, low to moderate grazing pressure and high nutrient levels within the euphotic zone. The model reproduces the correct succession of diatom and *E. huxleyi* blooms (Figure 15). A soon as average light intensities in the mixed layer are high enough during spring, diatom blooms develop first, the size and duration of which are limited by the amount of available silica in the mixed layer. *E. huxleyi* develops best at higher light intensities and therefore blooms later in the year. The magnitude but also the exact time of onset of *E. huxleyi* blooms are strongly determined by the amount of dissolved nitrate, which remains after the end of the preceding diatom bloom, and on the grazing pressure, which itself depends on the history of grazing populations. Note, that the model correctly reproduces the natural situation, that diatom blooms attain a higher chlorophyll biomass than the very small flagellate *E. huxleyi* (Figure 15). The maximum concentration of detached coccoliths in the water occurs after the period of maximum cell growth of *E. huxleyi*. This compares well to natural blooms, where satellite imagery and direct ship observations from the North Atlantic and Norwegian Fjord areas have shown, that the highest reflectivity in surface waters, which is caused by abundant detached coccoliths, is indicative for the latest phase of an *E. huxleyi* bloom.

4.2. Model results at different latitudes:

Figures 16 to 35 illustrate a set of results for the mixed layer from a simulation with COCDIA1004 over one year and at four different latitudes (35°N and 40°N, oligotrophic subtropical North Atlantic; 47°N, mesotrophic transitional North Atlantic; and 60°N, eutrophic subpolar North Atlantic). Input conditions for these four locations are illustrated for the light intensity, which penetrates the sea-surface (Figure 16), nutrients in the bottom layer (Figures 17 and 18), temperatures in the mixed layer (Figure 19) and the depth of the mixed layer (Figure 20). The calculated optical environment is summarized in Figures 21 to 25 (the depth of the euphotic zone, Figure 21; the light intensity in the mixed layer, Figure 22; the extinction coefficients for red, green and blue light in the mixed layer, Figure 25). The nutrient fields as a result of uptake due phytoplankton at these latitudes in the mixed layer are shown in Figure 26 (nitrate) and Figure 27 (silicate). The dynamics of diatom and *E. huxleyi* populations are shown in Figures 28 to 32. Simulated calcite production as a function of time and latitude by *E. huxleyi* are given in Figures 33 and 34, and organic carbon production (*E. huxleyi* plus diatoms) in Figure 35. These results show, that the model reproduces correctly the gradual increase of blooms with

increasing latitude for diatoms (Figure 28). In the case of *E. huxleyi* blooms occurred only at 47°N. The model failed to reproduce large blooms, such as were observed in nature at high latitudes. At 60°N for example, the predicted concentration in chlorophyll a for *E. huxleyi* is only 0.25 mg m^{-3}, whereas maximum chlorophyll concentrations during an extensive bloom of this species in the South Iceland Basin in 1991 have been of the order of 2 mg Chla m^{-3}. At this moment the reasons for this behaviour of the model is still enigmatic. Possible causes could be a too deep mixed layer during late spring/early summer. Monthly averaged seasonal and latitudinal variations of the mixed layer depths in the North Atlantic were parametrized from an oceanographic Atlas indicating 30m as a minimum value during summer stratification. Shipboard measurements during an *E. huxleyi* bloom in June 1991, however suggest, that the mixed layer thickness during an *E. huxleyi* bloom may be shallower than 20m also at high latitudes, which could at least partly explain these difficulties. Under these circumstances wind speeds, which are not included in the present model, could play a crucial role for a stable or rapidly fluctuating mixed layer, and hence could greatly enhance the chance for *E. huxleyi* bloom development.

Bloom development of *E. huxleyi* has also a strong influence on the annual production of coccolith calcite in the model. However, although earlier versions have been improved (integrating calcite production over the euphotic zone instead of the mixed layer, including a more realistic sub-model for temperature-dependent growth of *E. huxleyi*, removing dark-calcification and implementing a better nutrient model for the bottom layer) yearly coccolith calcite production is still too high, even after attaining steady state conditions during multi-year simulations. *E. huxleyi* calcite production predicted by the present model ranges from 2.5 to more than 40 gr calcite m^{-2} yr^{-1} (Figure 33), while from 11 sediment trap stations cited in the literature and from unpublished results the average global target value is about 1.4 gr coccolith calcite m^{-2} yr^{-1} (Figure 36).
In summary, although simple, the model is already capable to reproduce several aspects, that have been observed during *E. huxleyi* blooms at transitional latitudes. It does not yet allow to produce reliable maps of integrated calcite production of *E. huxleyi* in the North Atlantic. Suggested improvements to the model are:

1. Light: Include more realistic models for the underwater light-field and spectral characteristics for algal growth and calcification.
2. Temperature: Improve the seasonal temperature model by using parametrized values from the Robinson et al. (1979) atlas.
3. Vertical mixing: Improve the model for vertical mixing coefficients.
4. Grazing: Include a coupled preditor-prey system.

5. Export production: Describe food intake and excretion by zooplankton so, that the production of falling particles can be modelled explicitely. This would allow to describe the remineralization of calcite or organic matter more precisely.
6. CO_2: Include a subroutine, which describes the carbonate chemistry of the water.
7. Include CO_2/HCO_3^- uptake as a limiting nutrient for phytoplankton.
8. Change the layer structure of the model into a vertically continuous model structure by introducing local derivations of components with time and depth.

5. Literature:

Balch, W.M., Holligan, P.M., Ackleson, S.G., Voss, K.J., 1991. Biological and optical properties of mesoscale coccolithophore blooms in the Gulf of Maine. Limnology and Oceanography, 34 (4): 629-643.

Balch, W.M., Holligan, P.M., Kilpatrick, K.A., 1992. Calcification, photosynthesis and growth of the bloom-forming coccolithophore *Emiliania huxleyi.* Continental Shelf Research, 12 (12): 1353-1374.

Balch, W.M., Kilpatrick, K., Holligan, P.M., Cucci, T., 1993. Coccolith production and the detachment by *Emiliania huxleyi* (*Prymnesiophyceae*). Journal of Phycology, 29: 566-575.

Brand, L.E. and Guillard, R.R.L., 1981. The effects of continuous light and light intensity on the reproduction rates of twenty-two species of marine phytoplankton. Journal of Experimental Marine Biology and Ecology, 50: 119-132.

Brand, L.E., 1982. Genetic variability and spacial patterns of genetic differentiation in the reproductive rates of the marine coccolithophores *Emiliania huxleyi* and *Gephyrocapsa oceanica.* Limnology and Oceanography, 27 (2): 236-245.

Eppley, R.W., 1972. Temperature and phytoplankton growth in the sea. Fish. Bull. 70: 1063-1085.

Fisher, N.S., Honjo, S., 1991. Intraspecific differences in temperature and salinity responses in the coccolithophore *Emiliania huxleyi.* Biological Oceanography, 6: 355-361.

Goldman, J.C., and Carpenter, E.J., 1974. A kinetic approach to the effects of temperature on algal growth. Limnology and Oceanography, 19 (5): 756-766.

Henley, W.J., 1993. Measurement and interpretation of photosynthetic light-response curves in algae in the context of photoinhibition and diel changes. Journal of Phycology, 29: 729-739.

Jerlov, N.G., 1968. Optical oceanography. Elsevier Publishing Company Amsterdam, 194 p.

Mjaaland, G., 1956. Some laboratory experiments on the coccolithophorid *Coccolithus huxleyi.* Oikos, 7 (2): 251-255.

Robinson, M.K., Bauer, R.A., Schroeder, E.H., (1979). Atlas of North Atlantic-Indian Ocean. Monthly mean temperature and mean salinity of the mixed layer. Naval Oceanographic Office, Washington, D.C.

Sellers, W.D., 1965. Physical climatology. The University of Chicago Press, Chicago, 272 p.

Taylor, A.H., Watson, A.J., Ainsworth, M., Robertson, J.E., Turner, D.R., 1990. A modelling investigation of the role of phytoplankton in the balance of carbon at the surface of the North Atlantic. Global Biogeochemical Cycles, 5 (2): 151-171.

Van Bleijswijk, J.D.L., Kempers, R.S., Veldhuis, M.J., in press. Light dependent calcite carbon and organic carbon content of *Emiliania huxleyi* (*Prymnesiophyceae*).

Watabe, N. and Wilbur, K.M., 1966. Effects of temperature on growth, calcification, and coccolith form in *Coccolithus huxleyi*. Limnology and Oceanography, 11 (4): 567-575.

Webb, W.L., Newton, M., Starr, D., 1974. Carbon dioxide exchange of *Alnus rubra*. Oecologia (Berl.), 17: 281-291.

6. Figure captions:

Fig. 1: Scheme of the ecosystem for COCDIA 1004.

Fig. 2: Maximum specific growth rate (day^{-1}) of *E. huxleyi* at various temperatures as reported from the literature.

Fig. 3: Specific growth rate (day^{-1}) of *E. huxleyi* at 9 combinations of temperature and illumination as a function of nitrate (function GMAXE). Construction (365 days, DELTAT=0.05, nout=20):

Temperature	Light intensity		
	20 Wm^{-2}	50Wm^{-2}	100Wm^{-2}
7°C	Run #1	Run #4	Run #7
10°C	Run #2	Run #5	Run #8
28°C	Run # 3	Run #6	Run #9

Fig. 4: Comparison of published (with symbols) rates of calcification for *E. huxleyi* with modelled values as a function of irradiance.

Symbols:
Squares with dot=Balch et al., 1992 at 15°C; triangles=Balch et al., 1992 at 20°C; open circles=Balch et al., 1992 after addition of 2 µM nitrate; open squares=Balch et al., 1992 nitrate depleted; filled circles=Van Bleijswijk et al., 1994.

Model curves:
Run #1: CCMAX=28.9 Lith $cell^{-1}$ day^{-1}, RACC=0.04 $(Wm^{-2})^{-1}$
Run #2: CCMAX=28.9 Lith $cell^{-1}$ day^{-1}, RACC=0.0070682 $(Wm^{-2})^{-1}$
Run #3: CCMAX=18.1 Lith $cell^{-1}$ day^{-1}, RACC=0.0070682 $(Wm^{-2})^{-1}$

Fig. 5: Lith detachment model showing the rate of coccolith detachment (RDET, in Lith $cell^{-1}$ day^{-1}) as a function of the ratio of attached coccoliths divided by cell concentration (Q, in Lith $cell^{-1}$).

Fig. 6: Annual courses of the surface light intensity, which enters the watercolumn at 47°N at local noon (ISURF), and the light intensities in the mixed (IM) and thermocline (IT) layers in Wm^{-2}.

Fig. 7: Modelled daily solar radiation, which penetrates the sea-surface at 47°N from January 5 to 6.

Fig. 8: Average zonal radiation (Fig. 8.a), zonal energy loss terms (Fig. 8.b) and zonal atmospheric correction factors (Fig. 8.c) for COCDIA1004. Ca=Absorption of light by clouds, Cr=reflection and backscattering of light by clouds, Aa=absorption, of light by air molecules, dust and water vapour, Ar=reflection and scattering back to space by dry air molecules, dust and water vapour.

Fig. 9: Zonal (Figure 9.a) and seasonal (Figure 9 .b) variation of the sea-surface albedo in COCDIA 1004.

Fig.10: Example of annual courses of the temperatures (°C) in the mixed and thermocline layers modelled at 47°N.

Fig. 11: Parametrized seasonal variation of the mixed layer thicknesses between 35°N/20°W and 60°N/20°W (from Robinson et al., 1979). The thick line marks the situation at 47°N/20°W, which was test site for the model.

Fig. 12: Measured vertical profiles of nitrate in the Eastern North Atlantic (APNAP II and Dutch JGOFS cruises 1-4, Fig. 12.a) from sea-surface to 3000m depth. Fig. 12.b shows the same set of data for the interval between100m and 800m, that were used to linearly interpolate nitrate concentrations between different latitudes in the bottom layer.

Fig. 13: Distribution of linear coefficients a (Fig. 13.a) and b (Fig. 13.b) for the calculation of nitrate concentrations in the bottom layer (NB) as a function of latitude and time according to:

$$NB(Lat,time)=a(Lat) * Depth(time) + b(Lat),$$

and the calculated annual course of dissolved nitrate (NB) and silicate (SB) in the bottom layer at 47°N.

Fig. 14: Flow diagram of applications, data input and output for COCDIA1004, PPP400 and REDUCE2.

Fig. 15: Sample simulation of concentrations of diatoms (DM, mg Chla m^{-3}), *E. huxleyi* cells (PM, mg Chla m^{-3}), attached coccoliths (LAM, Liths m^{-3}) and isolated suspended coccoliths (LFM, Liths m^{-3}) at 47°N.

Example of a simulation run at 35°N, 40°N, 47°N, 50°N and 60°N with COCDIA1004 over one year:

Fig. 16: Surface irradiation penetrating the sea-surface (Wm^{-2}).
Fig. 17: Concentration of dissolved nitrate in the bottom layer ($mM\ m^{-3}$).
Fig. 18: Concentration of dissolved silicate in the bottom layer ($mM\ m^{-3}$).
Fig. 19: Temperature in the mixed layer as a function of time (°C).
Fig. 20: Depth of the mixed layer thickness as a function of time (m).
Fig. 21: Depth of the euphotic zone in comparison with the depth of the mixed layer thickness at 60°N.
Fig. 22: Distribution of the light intensity in the mixed layer as a function of time (Wm^{-2}).
Fig. 23: Development of extinction coefficients for red light in the mixed layer with time (m^{-1}).
Fig. 24: Development of extinction coefficients for green light in the mixed layer with time (m^{-1}).
Fig. 25: Development of extinction coefficients for blue light in the mixed layer with time (m^{-1}).
Fig. 26: Distribution of dissolved nitrate in the mixed layer as a function of time ($mM\ m^{-3}$).
Fig. 27: Distribution of dissolved silicate in the mixed layer as a function of time ($mM\ m^{-3}$).
Fig. 28: Diatom concentration in the mixed layer as a function of time ($mg\ Chla\ m^{-3}$).
Fig. 29: Specific growth rate of *E. huxleyi* in the mixed layer as a function of time (day^{-1}).
Fig. 30: Concentration of *E. huxleyi* cells in the mixed layer as a function of time ($mg\ Chla\ m^{-3}$).
Fig. 31: Concentration of attached coccoliths in the mixed layer as a function of time (10^{11} Liths m^{-3}).
Fig. 32: Concentration of detached coccoliths in the mixed layer as a function of time (10^{11} Liths m^{-3}).
Fig. 33: Cumulative vertically integrated calcite production rate as a function of time (gr calcite m^{-2}).
Fig. 34: Simulated annual and vertically integrated calcite production by *E. huxleyi* at various latitudes (gr calcite $m^{-2}\ yr^{-1}$).
Fig. 35: Simulated annual and vertically integrated organic C production by *E. huxleyi* and diatoms at various latitudes (gr org C $m^{-2}\ yr^{-1}$).
Fig. 36: Map showing the relative contribution of coccolith calcite fluxes to the total biogenic calcite fluxes in sediment traps from various sources in the literature.

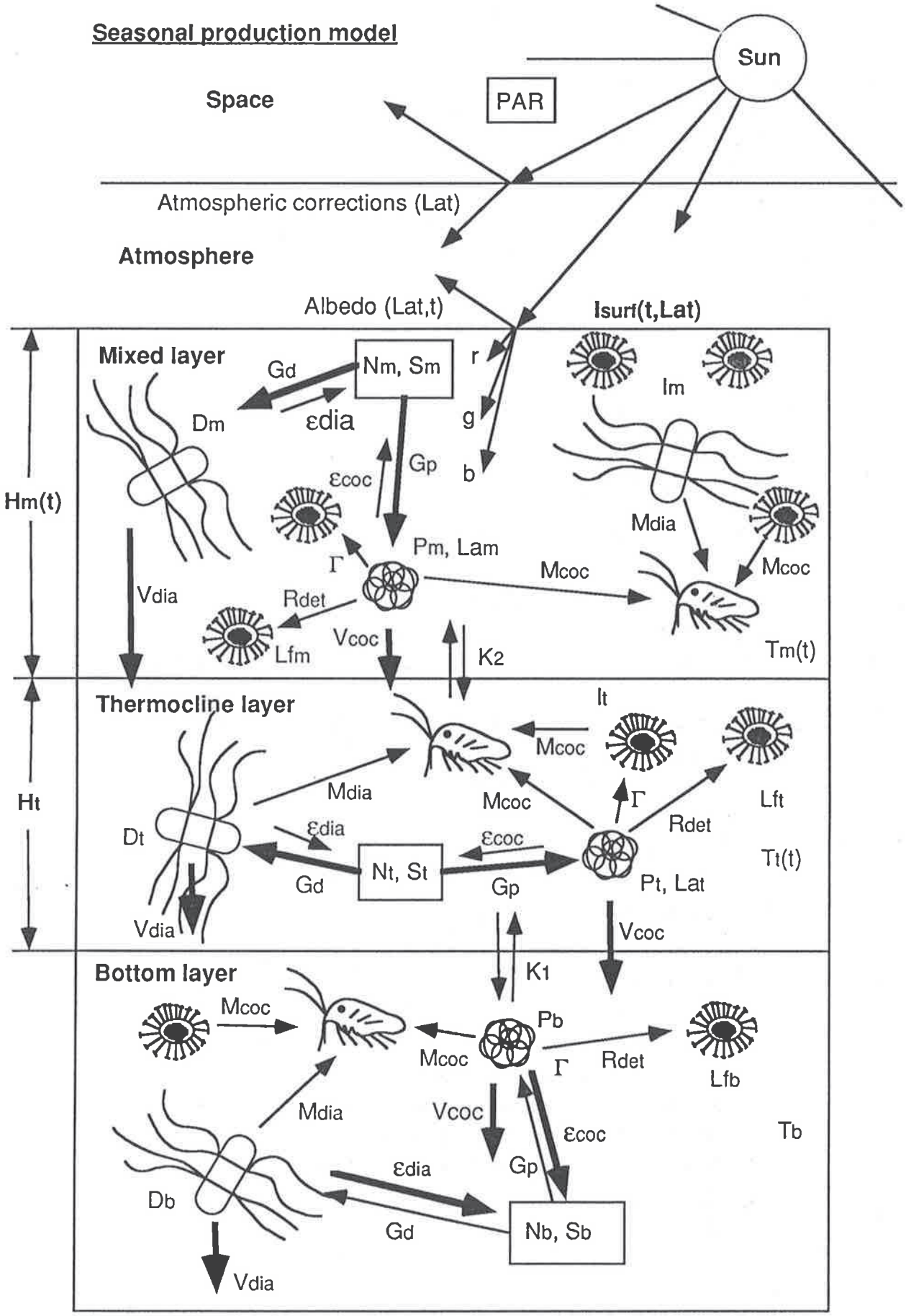
Seasonal production model
Sun
Space
PAR
Atmospheric corrections (Lat)
Atmosphere
Albedo (Lat,t)
Isurf(t,Lat)
Mixed layer
Nm, Sm
Gd
εdia
r
g
b
Dm
Im
εcoc
Gp
Hm(t)
Mdia
Pm, Lam
Γ
Mcoc
Mcoc
Vdia
Rdet
Lfm
Vcoc
K2
Tm(t)
Thermocline layer
It
Mcoc
Mdia
Mcoc
Γ
Lft
Rdet
Ht
Dt
εdia
εcoc
Nt, St
Gd
Gp
Pt, Lat
Tt(t)
Vdia
Vcoc
K1
Bottom layer
Mcoc
Pb
Mcoc
Γ
Rdet
Lfb
Mdia
Vcoc
εcoc
Tb
Gp
εdia
Db
Gd
Nb, Sb
Vdia

Figure 1

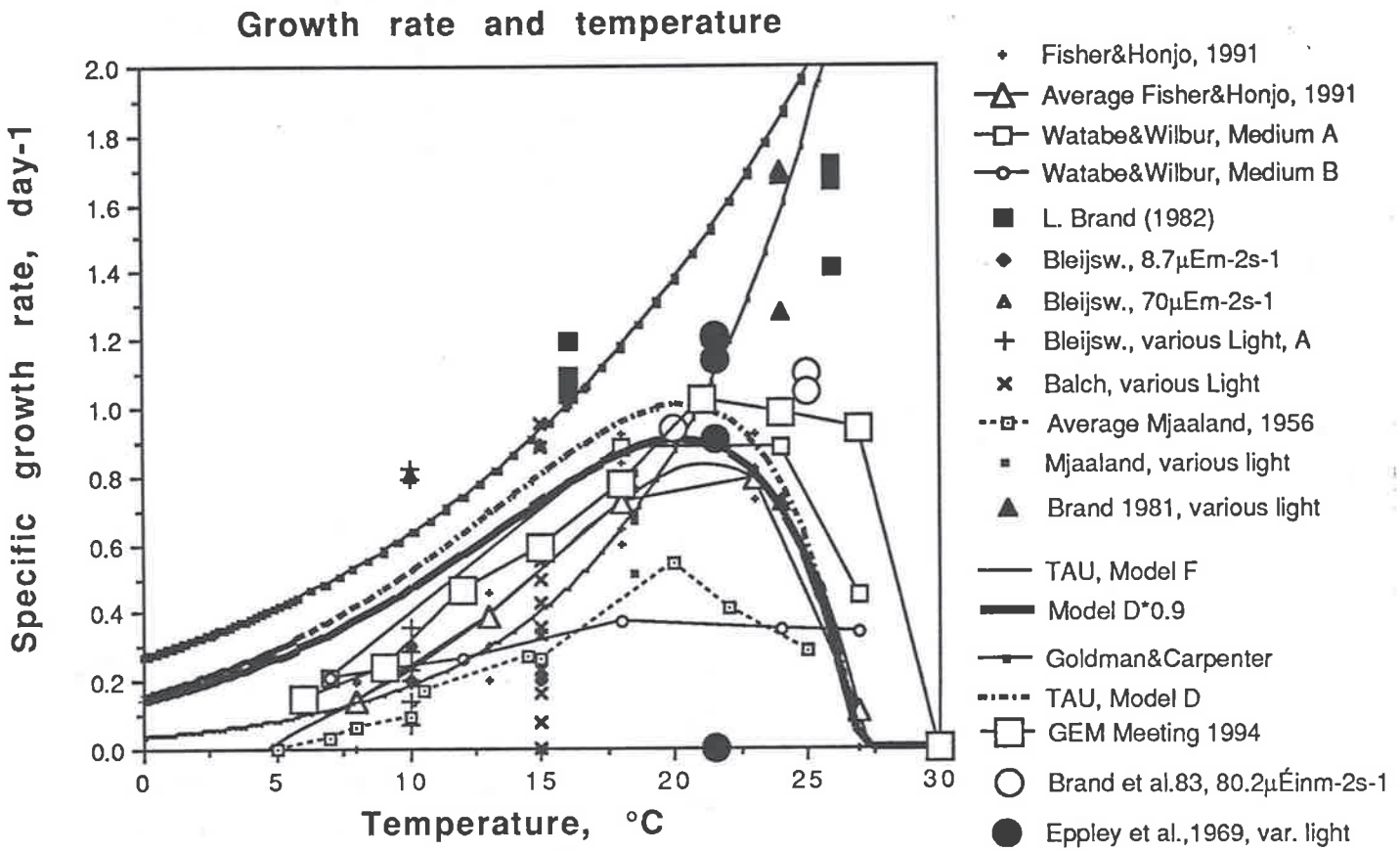
Growth rate and temperature
Specific growth rate, day-1
2.0
1.8
1.6
1.4
1.2
1.0
0.8
0.6
0.4
0.2
0.0
0
5
10
15
20
25
30
Temperature, °C
Fisher&Honjo, 1991
Average Fisher&Honjo, 1991
Watabe&Wilbur, Medium A
Watabe&Wilbur, Medium B
L. Brand (1982)
Bleijsw., 8.7µEm-2s-1
Bleijsw., 70µEm-2s-1
Bleijsw., various Light, A
Balch, various Light
Average Mjaaland, 1956
Mjaaland, various light
Brand 1981, various light
TAU, Model F
Model D*0.9
Goldman&Carpenter
TAU, Model D
GEM Meeting 1994
Brand et al.83, 80.2µÉinm-2s-1
Eppley et al.,1969, var. light

Fig. 2

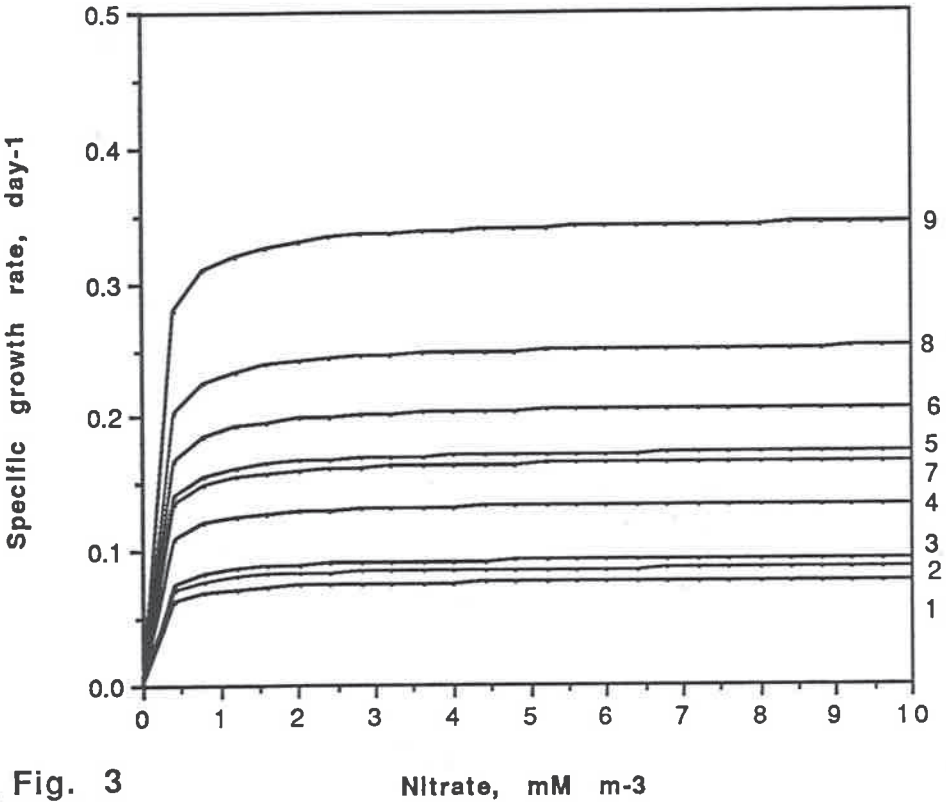

Fig. 3

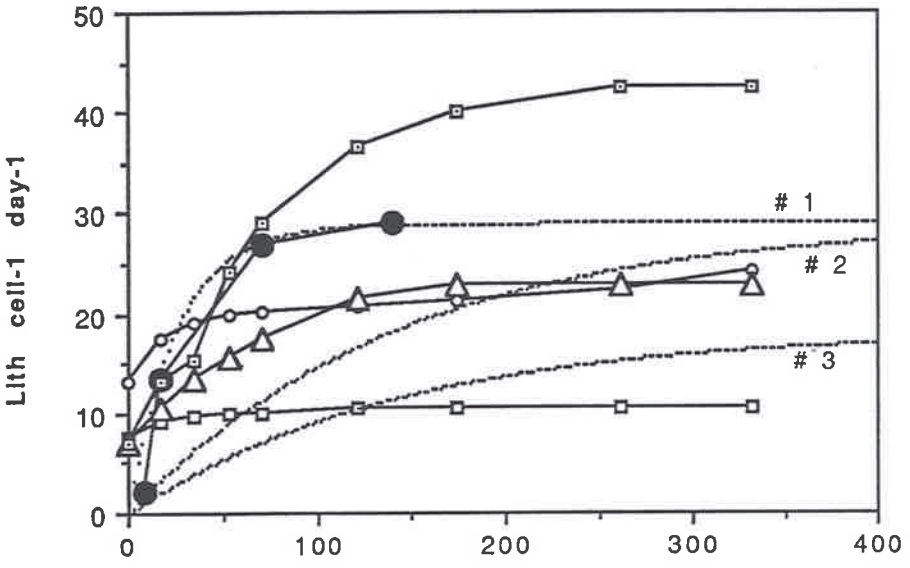

Fig. 4

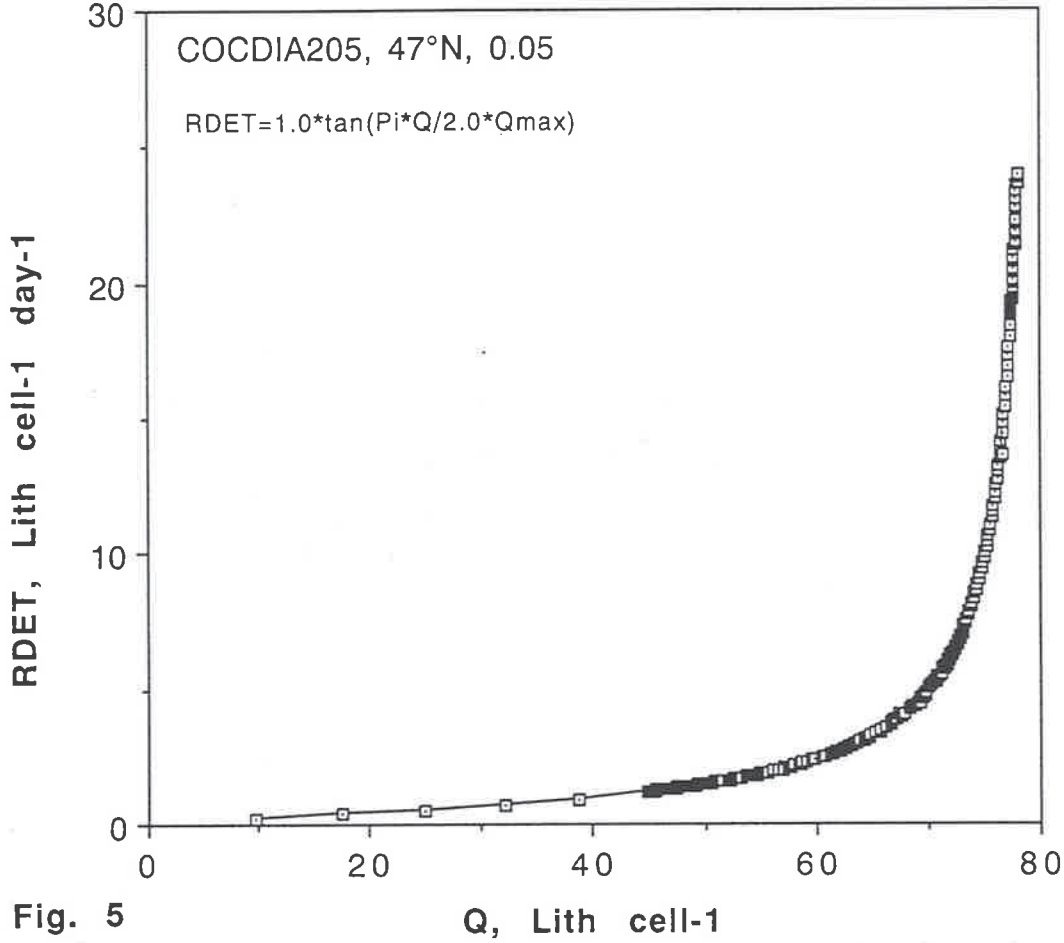

Fig. 5

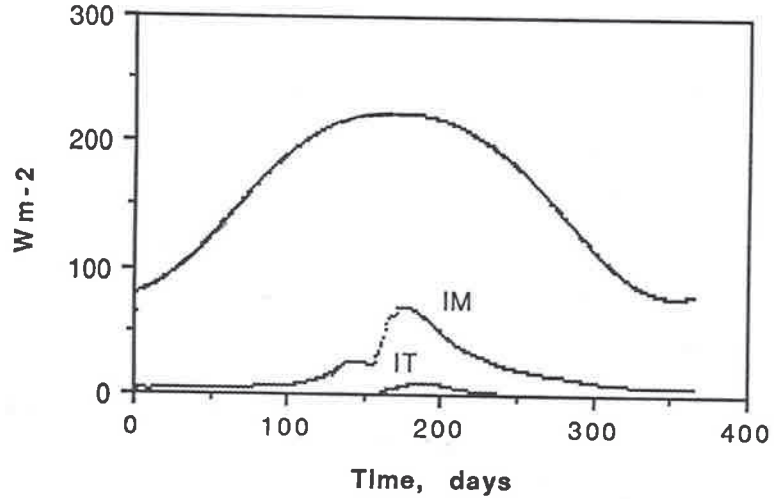
300
200
100
0
W m-2
IM
IT
0
100
200
300
400
TIme, days

Fig. 6

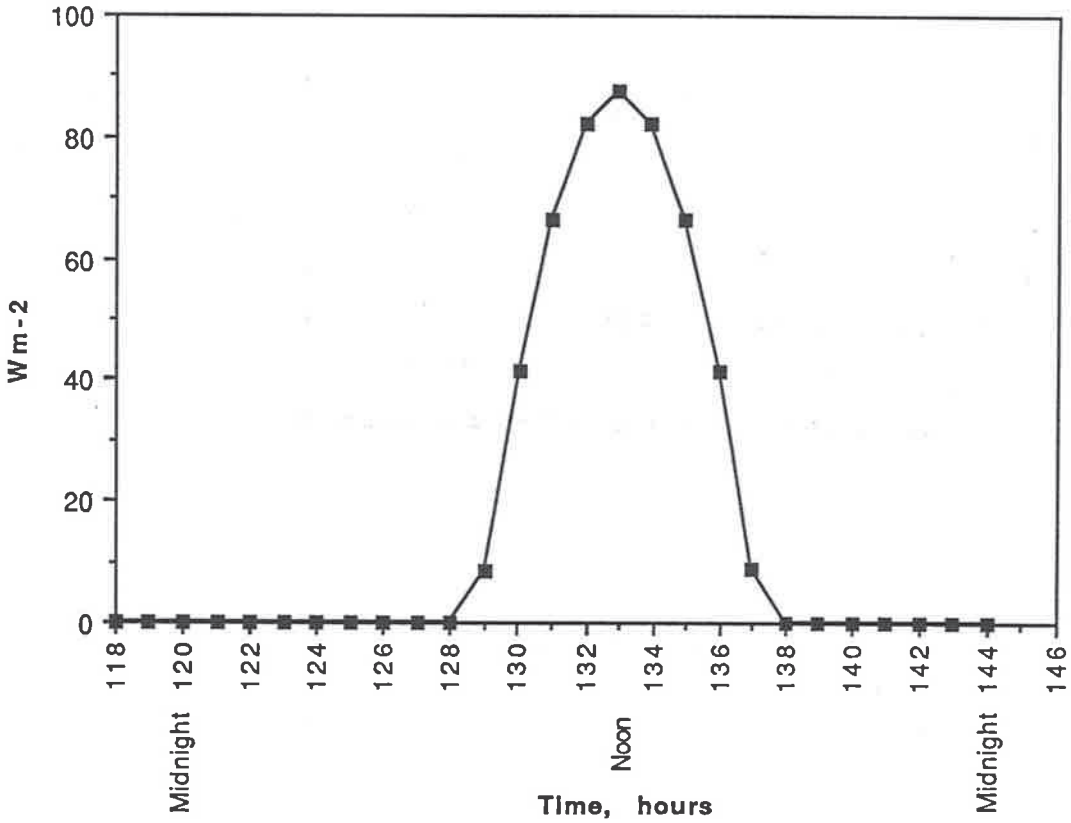
100
80
60
40
20
0
W m-2
118
120
122
124
126
128
130
132
134
136
138
140
142
144
146
Midnight
Noon
Midnight
TIme, hours

Fig. 7

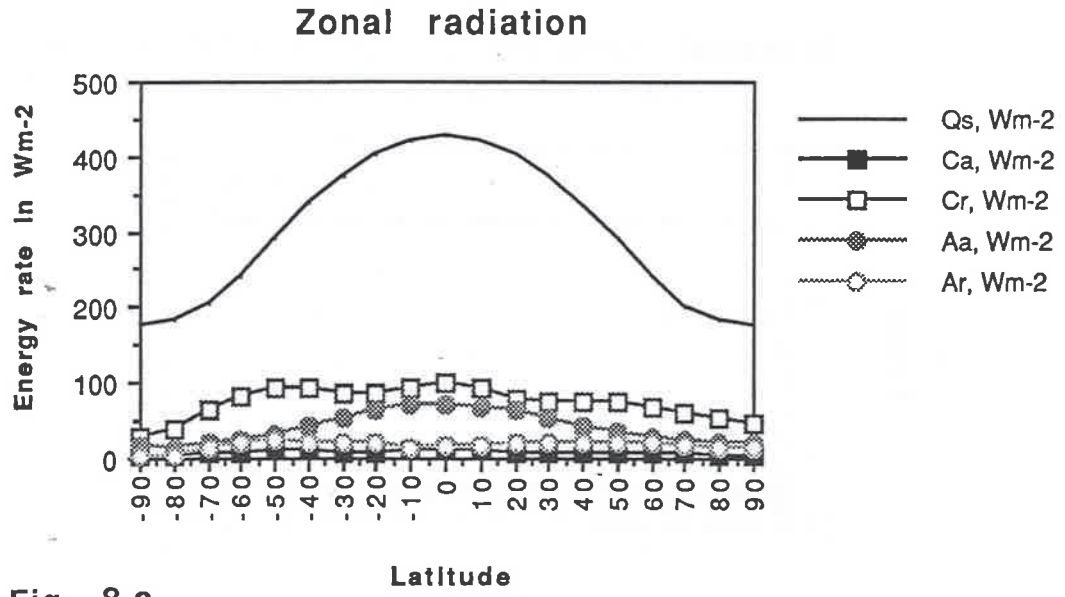

Fig. 8.a

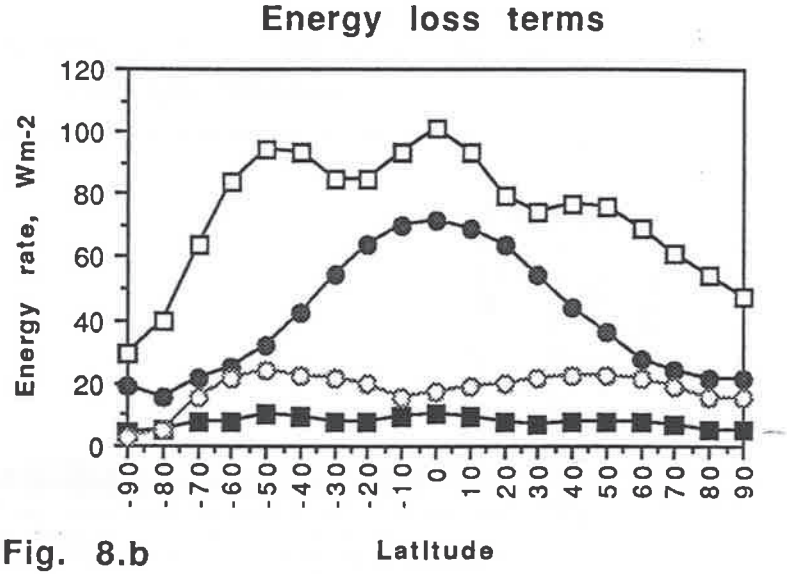

Fig. 8.b

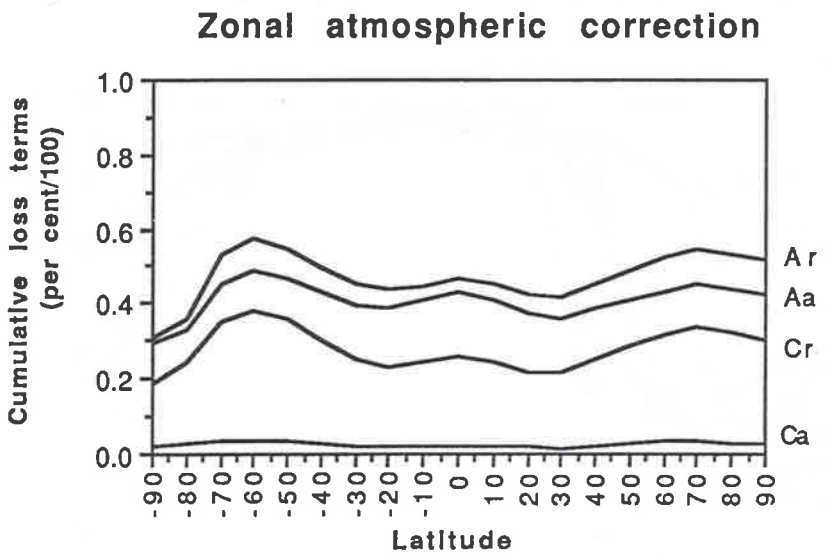

Fig. 8.c

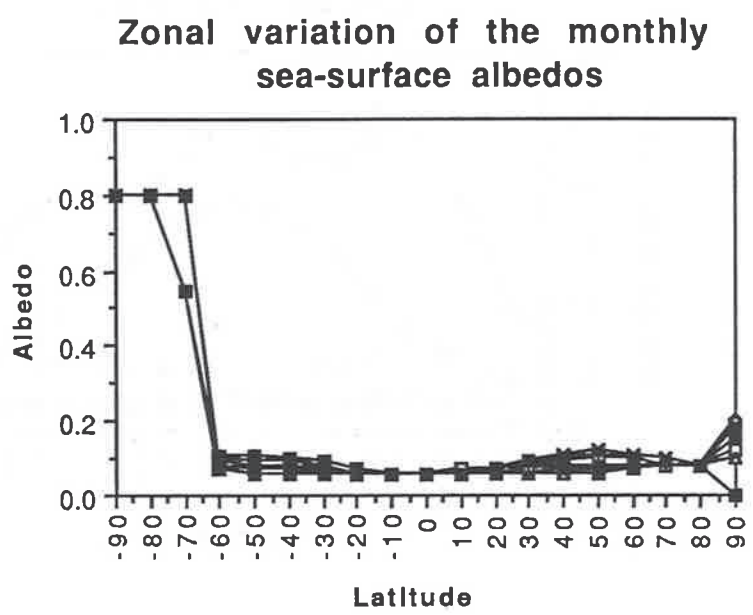

Fig. 9.a

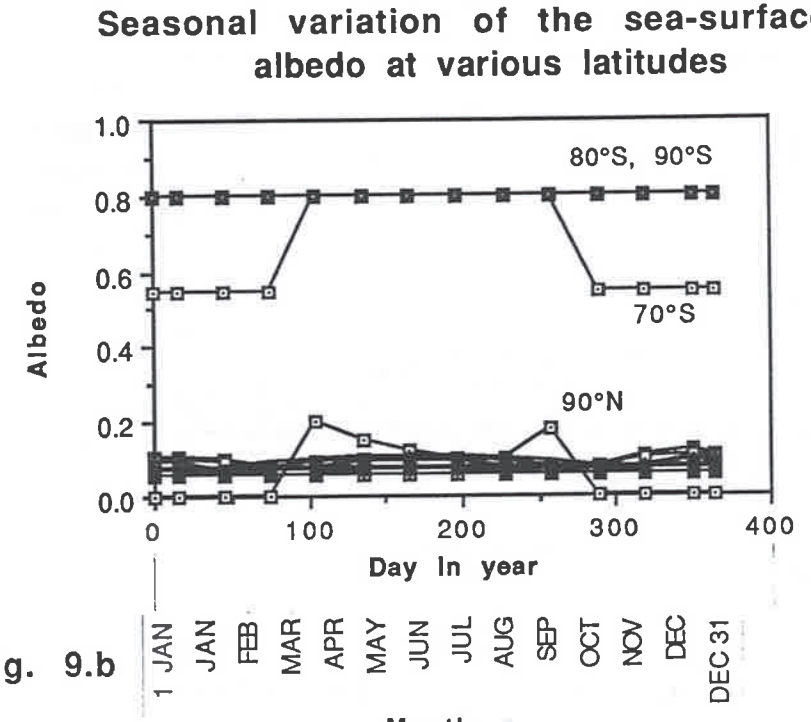

Fig. 9.b

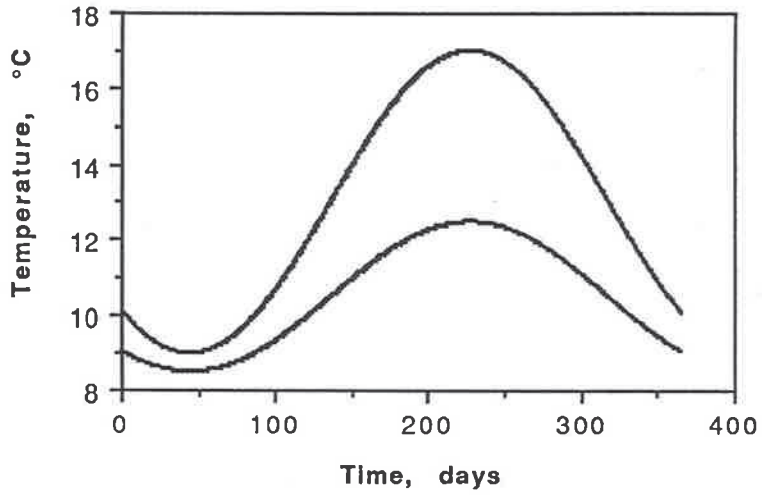

Fig. 10

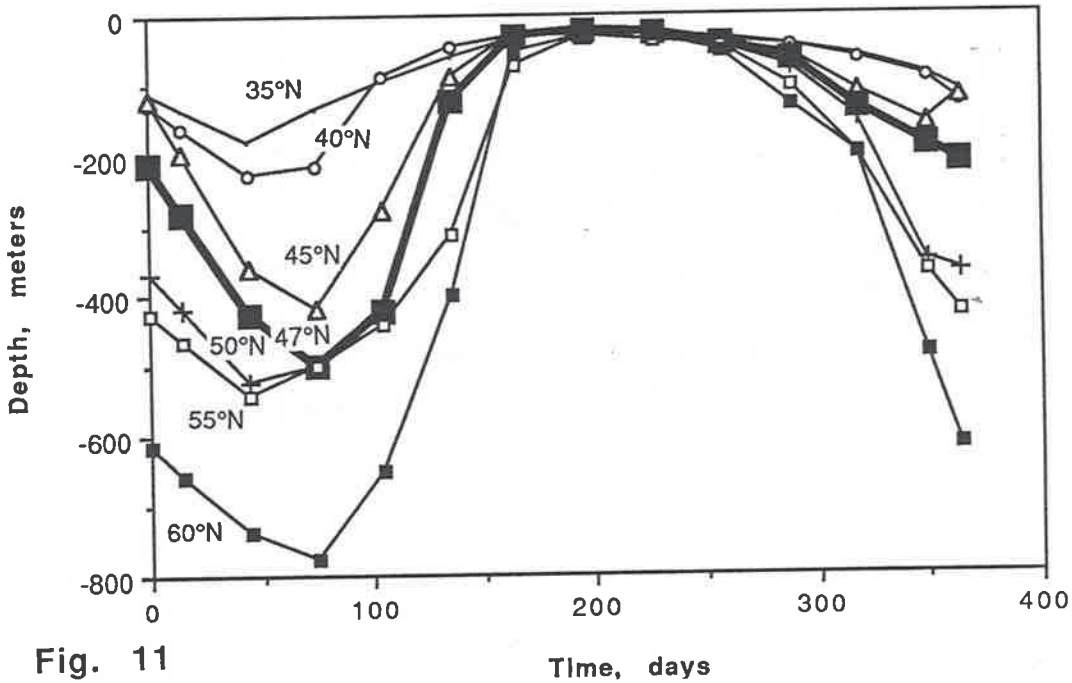

Fig. 11

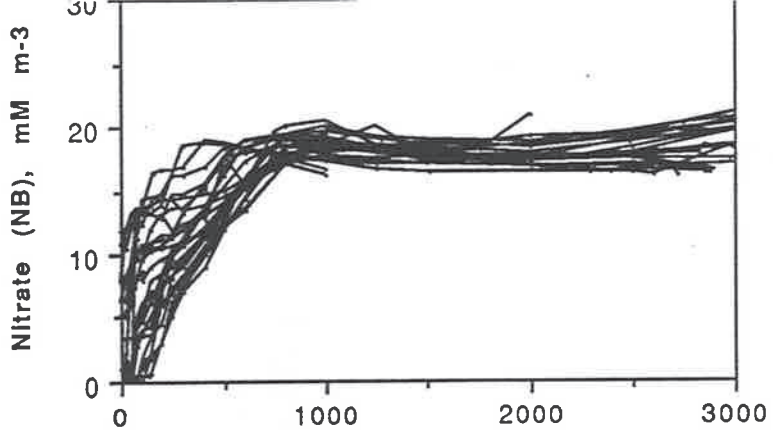

Fig. 12.a

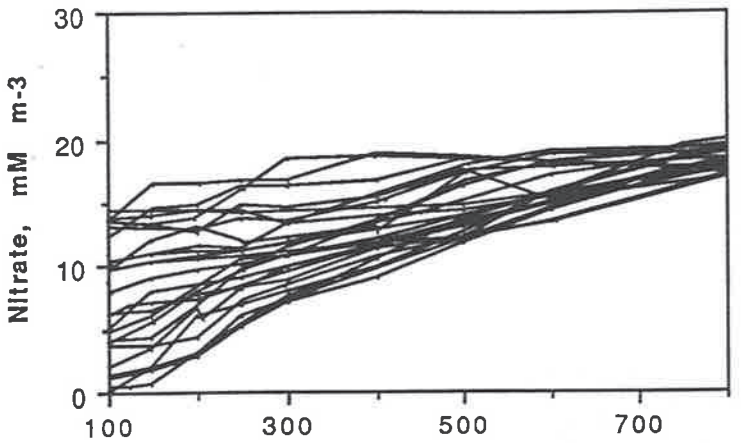

Fig. 12.b

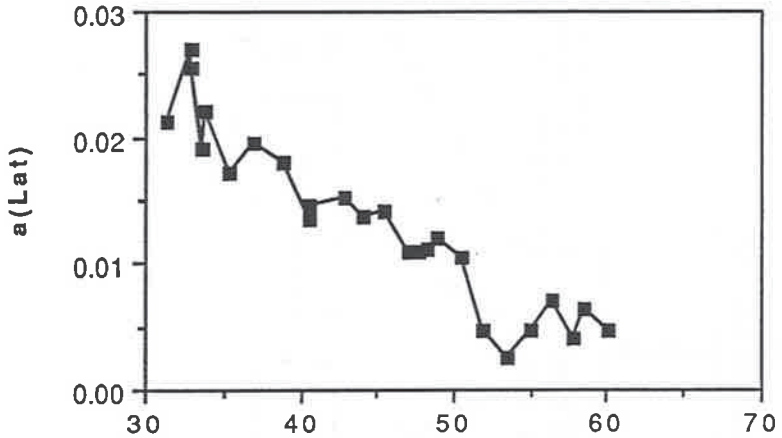

Fig. 13.a

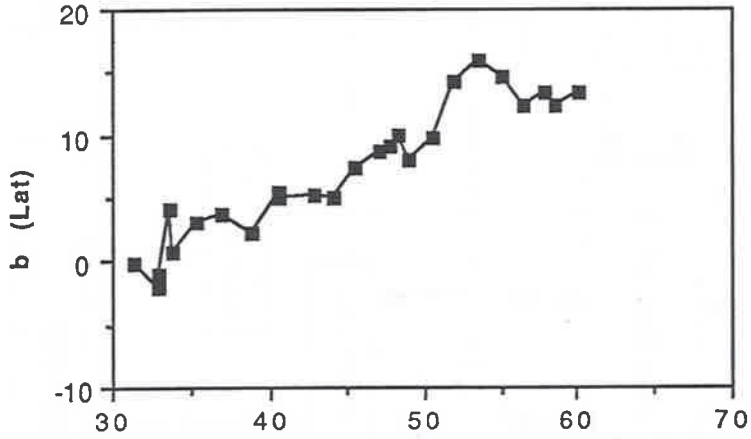

Fig. 13.b

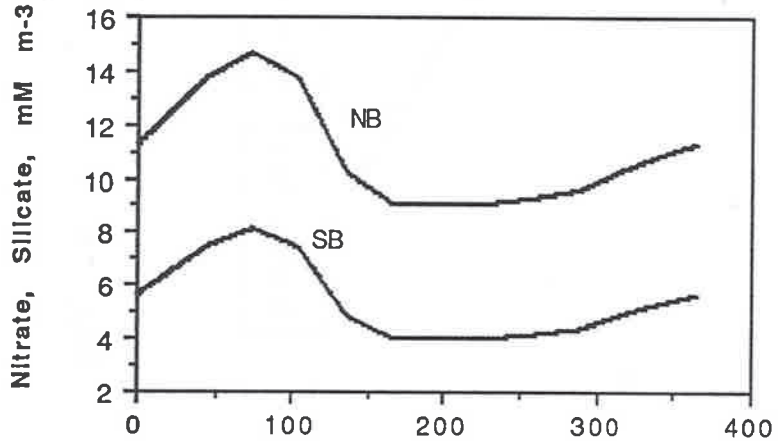

Fig. 13.c

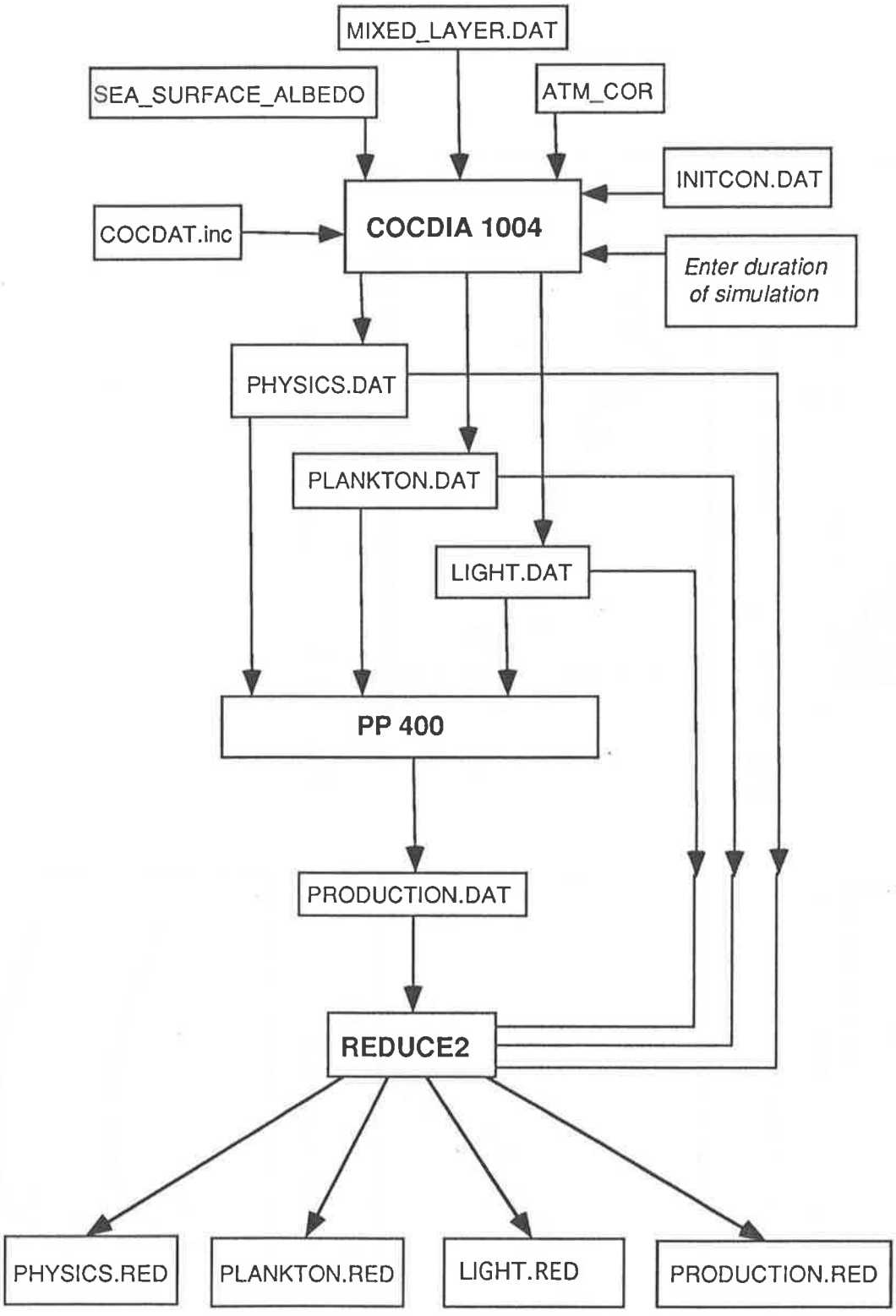
MIXED_LAYER.DAT
SEA_SURFACE_ALBEDO
ATM_COR
INITCON.DAT
COCDAT.inc
COCDIA 1004
Enter duration of simulation
PHYSICS.DAT
PLANKTON.DAT
LIGHT.DAT
PP 400
PRODUCTION.DAT
REDUCE2
PHYSICS.RED
PLANKTON.RED
LIGHT.RED
PRODUCTION.RED

Fig. 14

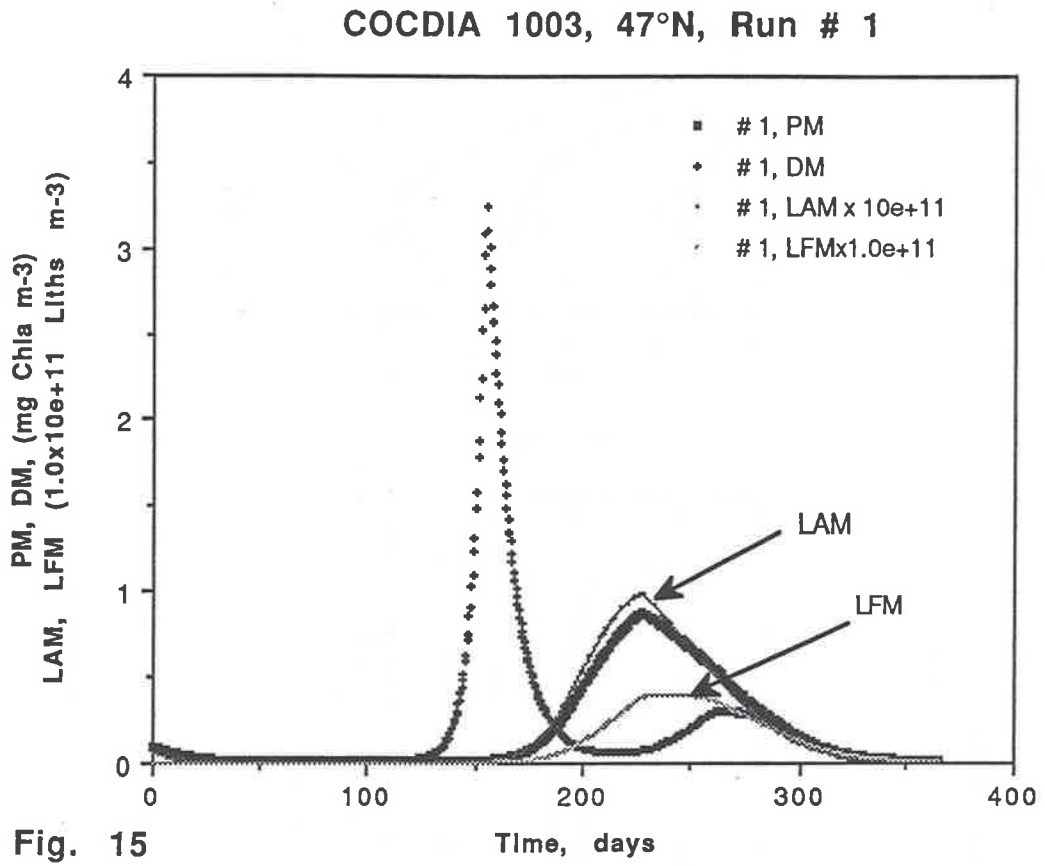
COCDIA 1003, 47°N, Run # 1
PM, DM, (mg Chla m-3)
LAM, LFM (1.0x10e+11 Lths m-3)
1, PM
1, DM
1, LAM x 10e+11
1, LFMx1.0e+11
LAM
LFM
0
1
2
3
4
0
100
200
300
400
Time, days

Fig. 15

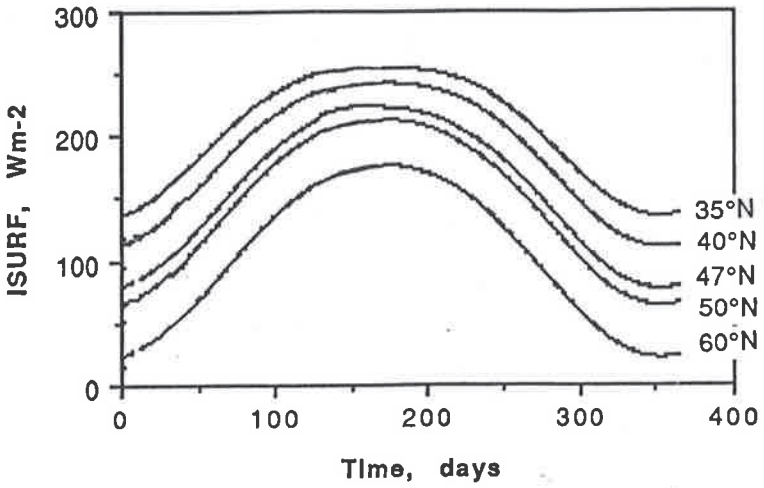

Fig. 16

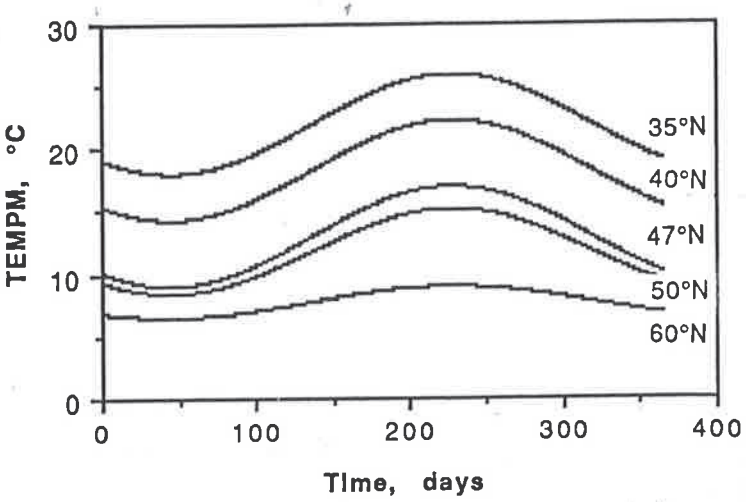

Fig. 19

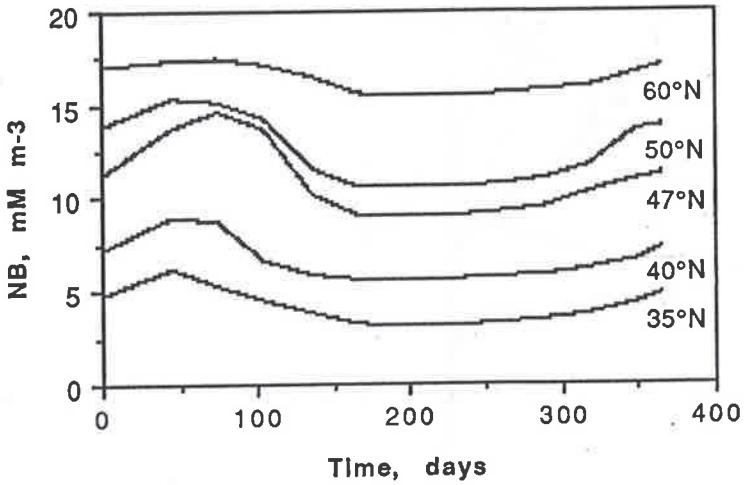

Fig. 17

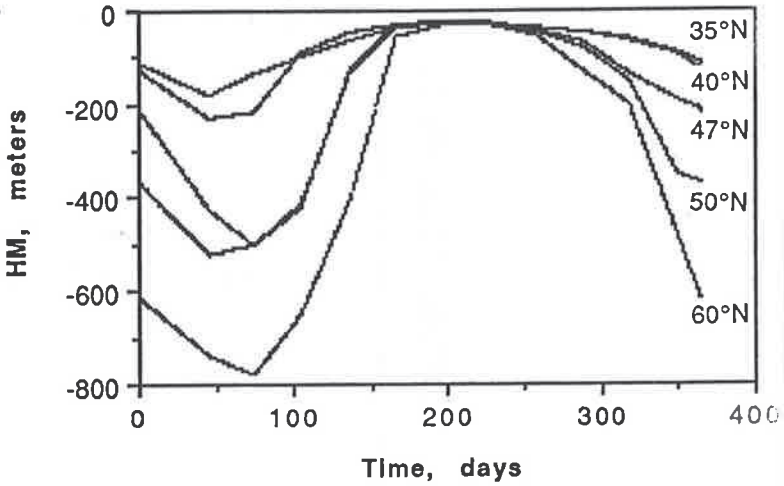

Fig. 20

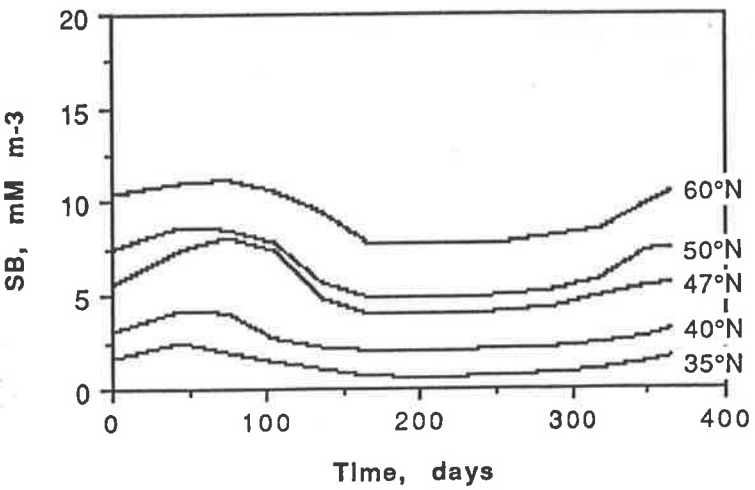

Fig. 18

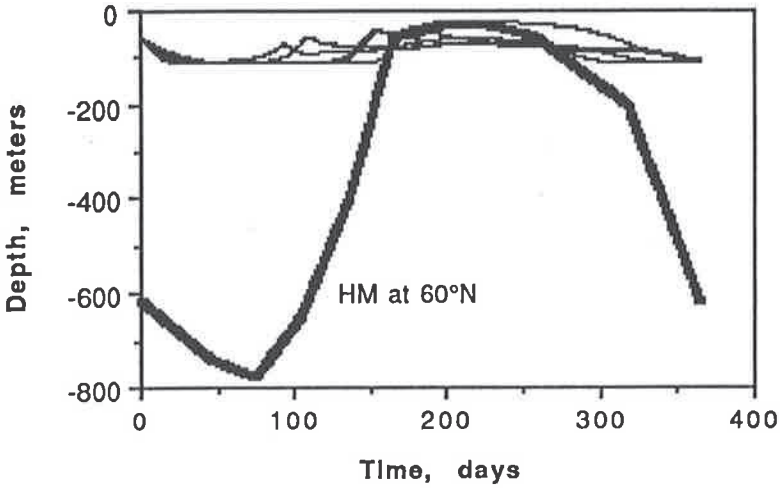

Fig. 21

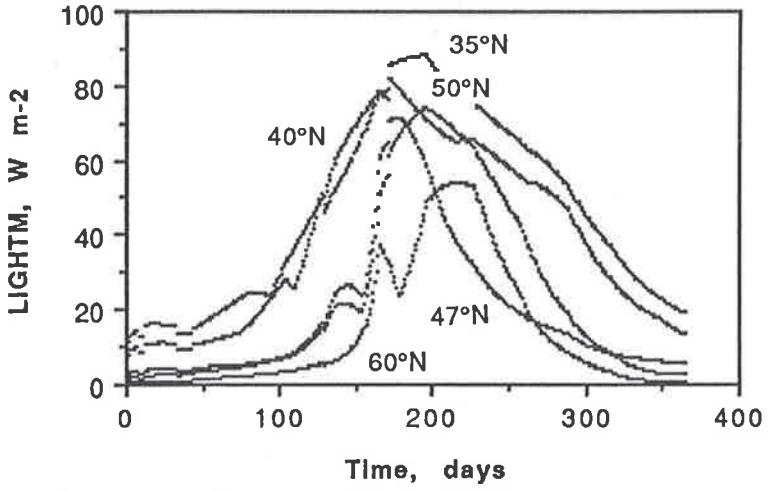

Fig. 22

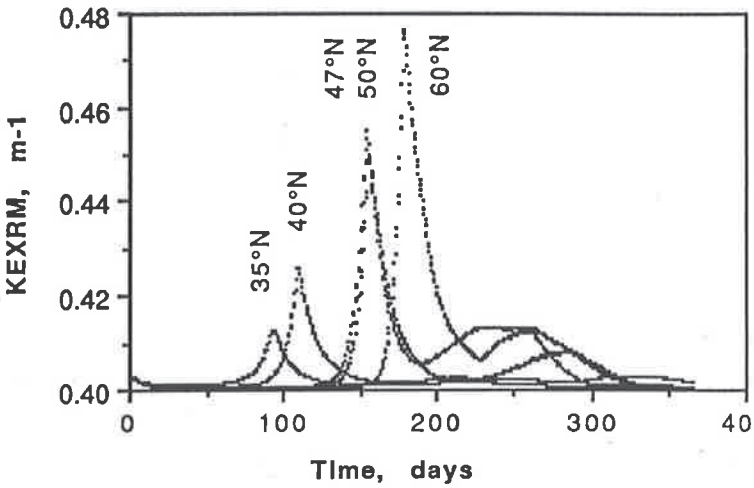

Fig. 23

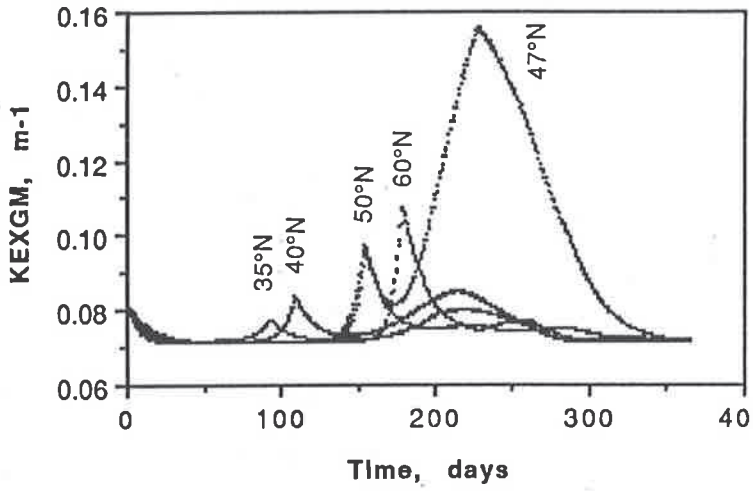

Fig. 24

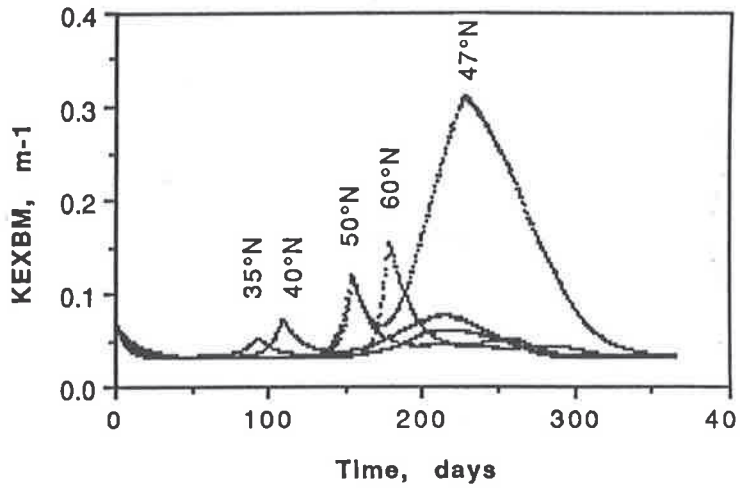

Fig. 25

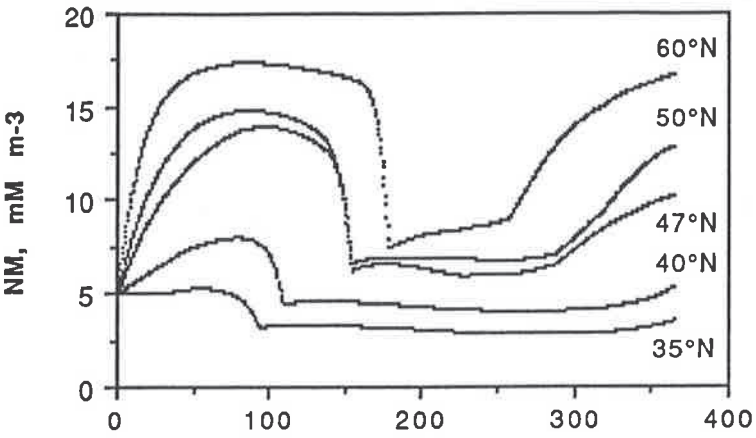

Fig. 26

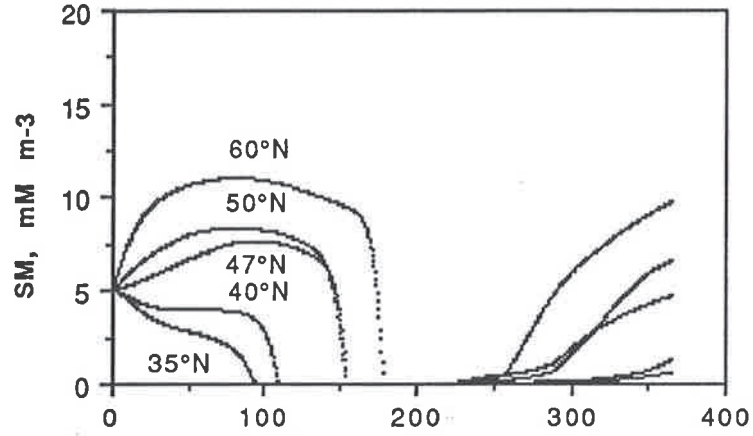

Fig. 27

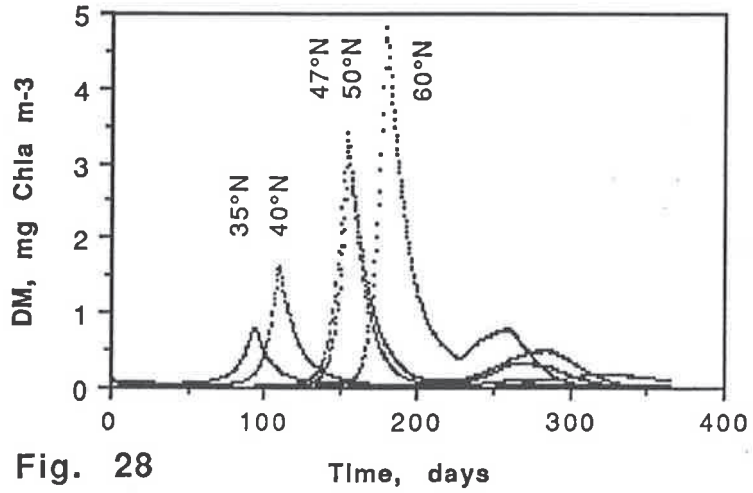

Fig. 28

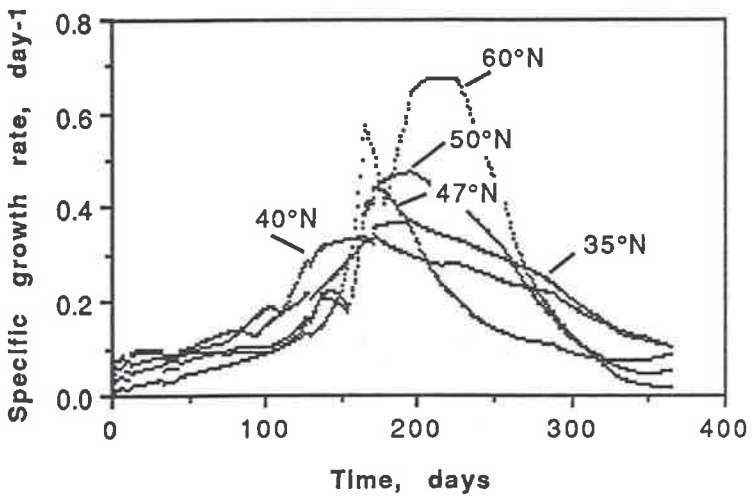

Fig. 29

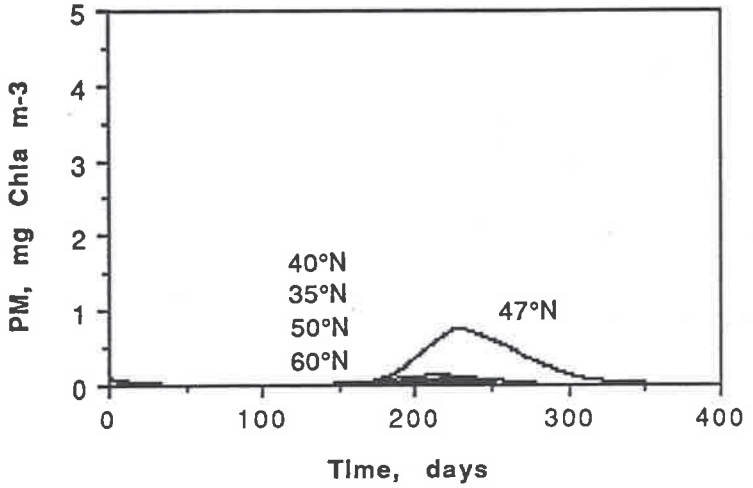

Fig. 30

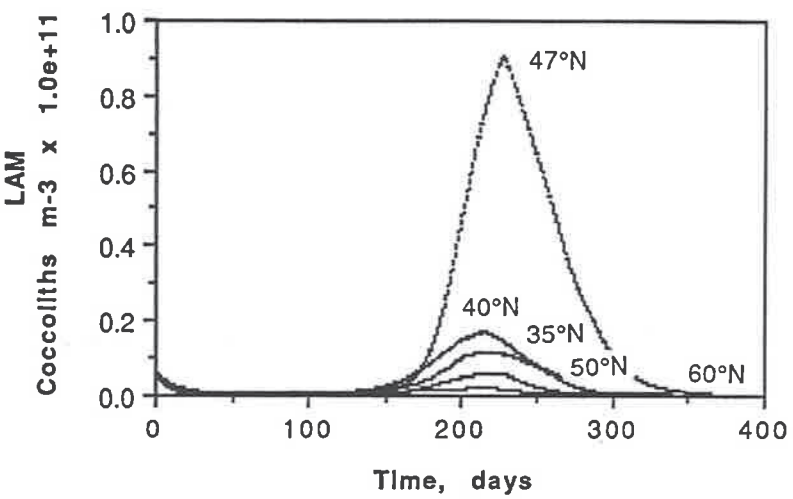

Fig. 31

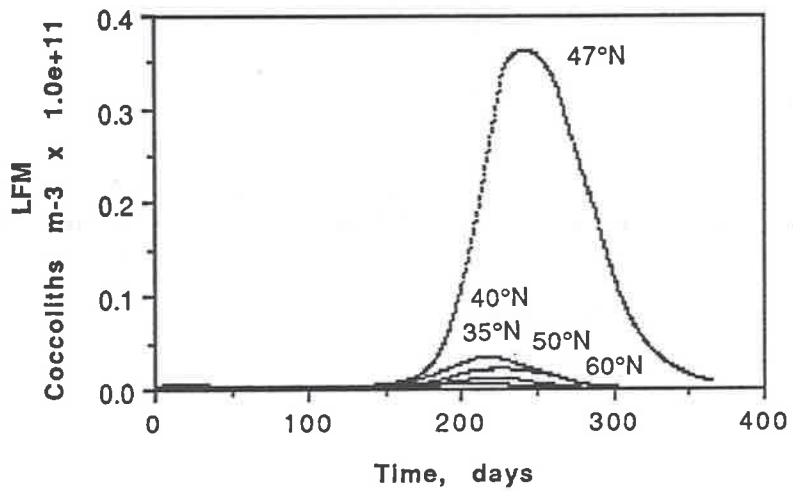

Fig. 32

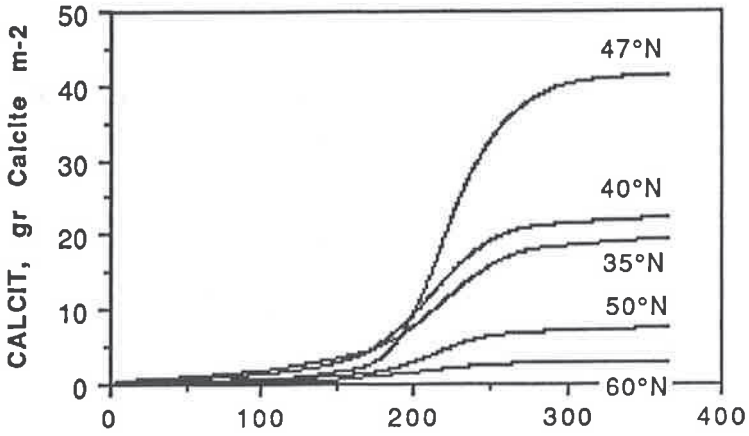

Fig. 33

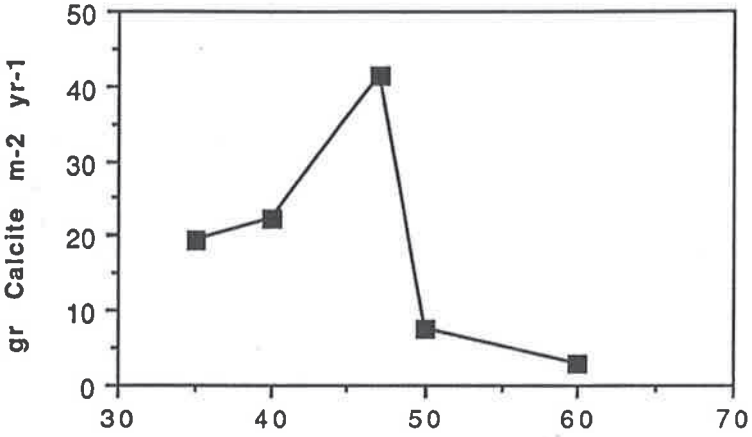

Fig. 34

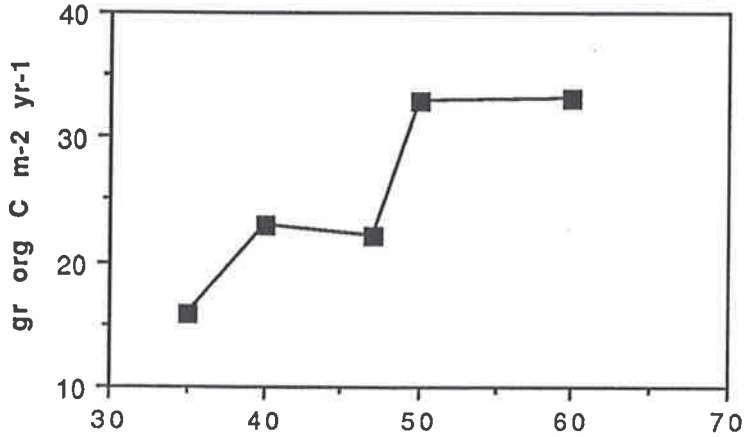

Fig. 35

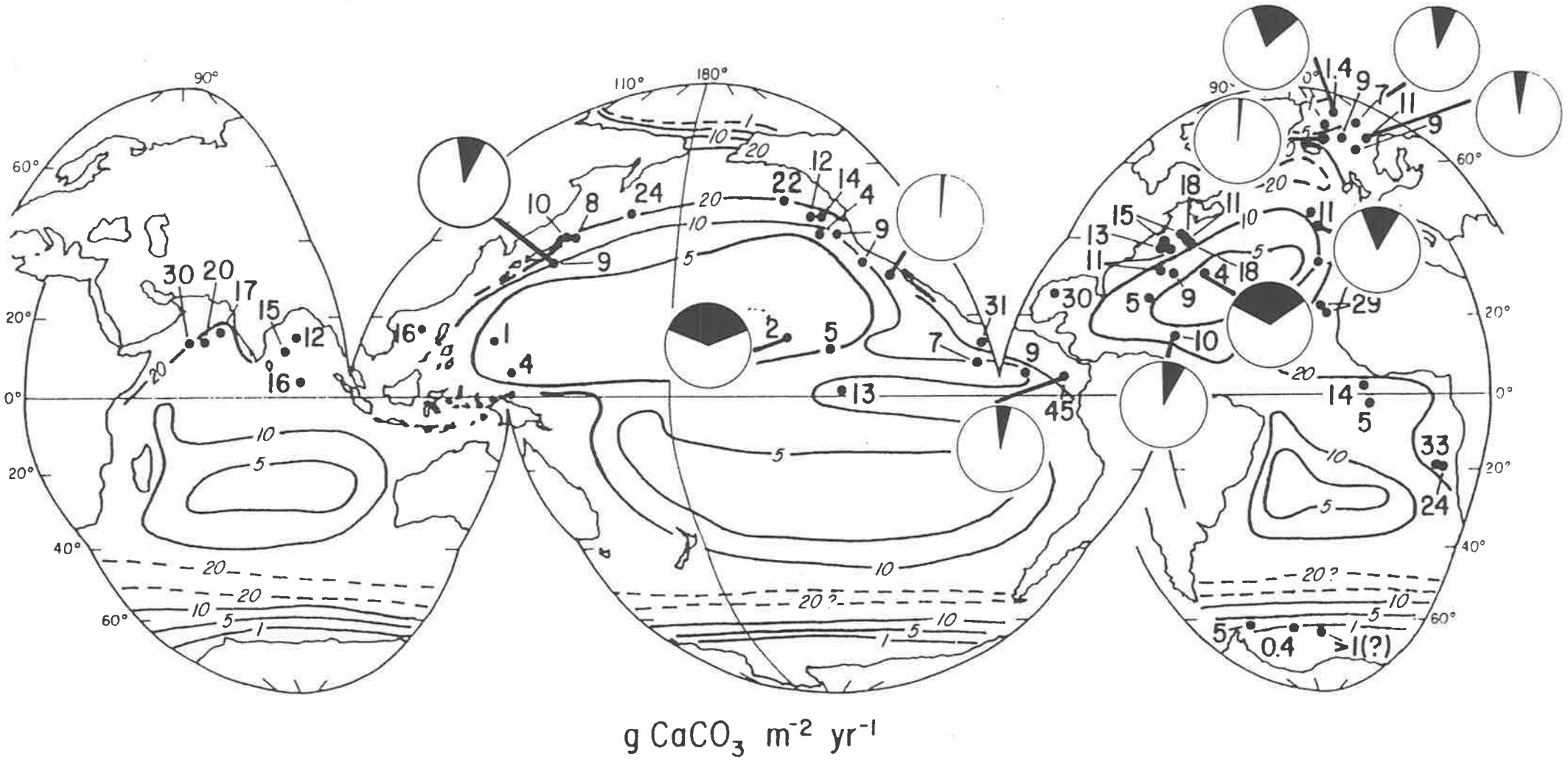

Comparison of average coccolith calcite fluxes (black) with total calcite fluxes (=100%) from various sediment trap locations. Map of total calcite fluxes from Milliman, J.D. (1993) Global Biogeochemical Cycles, **7**, 927-957. Coccolith flux estimates are based on data from Honjo, 1978; Steinmetz, 1990; Samtleben & Bickert, 1990; Knappertsbusch & Brummer, in press; Ziveri et al., in press; Andruleit et al., in press., Okada, 1994.

Fig. 36